2015

Limpet shells as unmodified tools in Pleistocene Southeast Asia: an experimental approach to assessing fracture and modification

Katherine A. Szabo
University of Wollongong, kat@uow.edu.au

Brent Koppel
University of Wollongong, bk830@uowmail.edu.au

Publication Details

Szabo, K. & Koppel, B. (2015). Limpet shells as unmodified tools in Pleistocene Southeast Asia: an experimental approach to assessing fracture and modification. Journal of Archaeological Science, 54 64-76.

Limpet shells as unmodified tools in Pleistocene Southeast Asia: an experimental approach to assessing fracture and modification

Abstract
Pleistocene tools manufactured in shell are rarely identified. This may in part be due to the complexity of shell as a raw material and associated challenges in recognising and interpreting shell modification. A series of unusually-shaped Scutellastra flexuosa limpets from c. 30,000 year old deposits in Golo Cave, eastern Indonesia were identified as putatively modified during midden analysis. A pilot programme of investigations into the microstructure and natural fracture patterns of this species, coupled with a series of use-wear experiments, demonstrates that some S. flexuosa shells were used as scrapers. The shells were used in unmodified form and were 'repurposed' after having been gathered for subsistence purposes. Taken together with other forms of early shell-working already reported for Golo Cave, the identification of these new unmodified shell tools expands the corpus of shell tool use at the site and presents a picture of diversity and complexity not seen in the associated lithic assemblage.

Disciplines
Medicine and Health Sciences | Social and Behavioral Sciences

Publication Details
Szabo, K. & Koppel, B. (2015). Limpet shells as unmodified tools in Pleistocene Southeast Asia: an experimental approach to assessing fracture and modification. Journal of Archaeological Science, 54 64-76.

Limpet shells as unmodified tools in Pleistocene Southeast Asia: an experimental approach to assessing fracture and modification

Katherine Szabó* and Brent Koppel

Centre for Archaeological Science, University of Wollongong, Wollongong NSW 2522, Australia

*Corresponding author: kat@uow.edu.au +61 2 4221 5846

Abstract

Pleistocene tools manufactured in shell are rarely identified. This may in part be due to the complexity of shell as a raw material and associated challenges in recognising and interpreting shell modification. A series of unusually-shaped *Scutellastra flexuosa* limpets from c. 30,000 year old deposits in Golo Cave, eastern Indonesia were identified as putatively modified during midden analysis. A pilot programme of investigations into the microstructure and natural fracture patterns of this species, coupled with a series of use-wear experiments, demonstrates that some *S. flexuosa* shells were used as scrapers. The shells were used in unmodified form and were 'repurposed' after having been gathered for subsistence purposes. Taken together with other forms of early shell-working already reported for Golo Cave, the identification of these new unmodified shell tools expands the corpus of shell tool use at the site and presents a picture of diversity and complexity not seen in the associated lithic assemblage.

Keywords

Limpet shells, *Scutellastra flexuosa*, shell tools, Pleistocene, Southeast Asia

Introduction

Molluscan shell used as a raw material for tool production is uncommonly noted for Pleistocene archaeological assemblages in different global locations. Active modification of molluscs for use – typically as scrapers – has been noted for a number of coastal Mousterian sites in Italy and Greece (Douka and Spinapolice 2012; Stiner 1994). Choi and Driwantoro (2007) argued for the use of shell knives by Javanese *Homo erectus*, however fundamental problems with the argument (outlined in Szabó 2013) means that these tools will be discounted here. For *Homo sapiens*, the deliberate modification of the large, calcareous

opercula of *Turbo marmoratus* was reported at c. 32,000 – 28,000 BP for eastern Indonesia (Szabó et al. 2007), and preliminary observations of other contemporaneous types of shell working and modification at the same site were also made. It is one of these other putative forms of shell tool – the use of unmodified *Scutellastra flexuosa* limpets as scrapers – that we investigate here.

The behaviour of shell as a raw material for artefact production is poorly understood. Different molluscan families can have profoundly different microstructures, and thus structural properties (Currey and Taylor 1974; Watabe 1988). Taphonomic processes, including recrystallization of the calcium carbonate building blocks and the degradation of the protein fraction which composes the matrix in which crystals are enmeshed, further complicate the responses of shells to force. Given these various properties, diagnostic patterns of fracture in lithic materials are a poor analogue for understanding the behaviour of shell, and new methods through which to recognise and interpret shell-working and modification are needed.

Using a programme of experimental use-wear replication, as well as investigations into the structural nature and taphonomic proclivities of *S. flexuosa* limpets, we pilot a technique to help discern between (1) natural breakage and taphonomic modification, and (2) cultural patterns of surface and edge modification through use of the shells as unmodified tools. If demonstrated, ~30,000 year old use of shell as a raw material would include not only the focussed gathering and structured reduction of *Turbo marmoratus* opercula (Szabó et al. 2007), but the repurposing of shell midden refuse for use as expedient tools.

Background to the site and sample

Golo Cave is limestone solution cave located on Gebe Island, northern Maluku, eastern Indonesia (see Figure 1). Excavations of a 5 x 1 metre trench and two separate 1 x 1 metre squares to bedrock in 1994 and 1996 by Bellwood and colleagues uncovered stratified archaeological deposits spanning from 32 kya just above bedrock to the uppermost deposits associated with the Southeast Asian Metal Age (~2 kya) (Bellwood *et al.* 1998) (see Table 1). Along with the analogous and nearby Wetef Cave (Irwin et al. 1999), Golo Cave presents a punctuated early modern human sequence on a small, resource-poor island that was not landbridged to the west (Halmahera) or east (New Guinea) during periods of lower sea level. Thus, not only does it encapsulate early modern human abilities in terms of its successful colonisation, but also the adaptive flexibility of its colonists who readily used bone and shell to complement the poor lithic resources (Pasveer and Bellwood 2004; Szabó et al. 2008) and translocated marsupial fauna from neighbouring New Guinea to generate hunting stock (Flannery et al. 1998).

In addition to animal bone (Flannery et al. 1998), bone tools (Pasveer and Bellwood 2004) and lithic artefacts (Szabó et al. 2007), quantities of shell midden were recovered from throughout the cultural sequence. A total sample of midden shell from one excavated

square (M4) was transported to the Australian National University, and subsequently the University of Wollongong, for further analysis and all shell discussed here derives from this square.

A total of 1064 individuals (MNI) from fifty-seven different molluscan species was identified, with most of these species being represented by a single individual (see Table 2). Eight percent (MNI = 92) were terrestrial snails belonging to a variety of species which are most likely self-introduced into the deposits. A further one percent (MNI = 10) derive from soft-shore intertidal habitats. Ninety-one percent of the individuals are from hard-substrate habitats, with two percent from the reef-flat intertidal zone, but the vast majority (89% MNI = 942) were collected from upper intertidal and 'splash zone' rocks. These molluscs would have been accessible regardless of tidal activity providing a consistent and easily visible resource.

Three species of limpet comprise seventy-eight percent (MNI = 691) of the upper intertidal assemblage: *Cellana radiata* (Nacellidae)(MNI = 407), *Patelloida striata* (Lottiidae)(MNI = 206) and *Scutellastra* (=*Patella*) *flexuosa* (Patellidae)(MNI = 78)(see Figure 2). The dominance of limpets is particularly pronounced within the earliest deposits, with *C. radiata* comprising forty percent of the assemblage recovered from below 175 cm, *C. striata* comprising twenty-one percent, and all of the *S. flexuosa* being found below this depth. There were certainly other nearshore marine habitats present in the earliest phases of occupation, as demonstrated by the presence of subtidal lagoonal species such as *Turbo marmoratus* sourced for artefact production at Golo (Szabó et al. 2008), but there was a clear focus for subsistence gathering on the upper intertidal zone.

During the course of midden analysis, it was noted that some of the *S. flexuosa* shells were missing portions of the crenulate margin (Figure 3). Rather than these areas having an abrupt and angular edge characteristic of compression fracture caused by a process such as trampling, the edges were rounded suggesting modification through abrasion. None of the remaining surfaces of these highly-sculptured shells showed evidence of abrasion, and this localised wear was hypothesized to represent deliberate human use in a scraping or cutting motion.

To test this idea, a programme of experimental work was set up to delineate the natural breakage patterns of *S. flexuosa* under various forces as well as any modifications characteristic of the working of a range of material textures in different ways. All *S. flexuosa* specimens identified from the shell midden assemblage were analysed using a low-power stereo microscope and those that showed possible or putative signs of deliberate cultural modification were separated for further analysis.

Framework for investigation

As a biomaterial whose primary function is to protect soft-bodied molluscs from predators, shells are adaptively designed to be strong in particular directions to resist crushing and impact forces (Vermeij 1993). Feature of macrodesign, including curvature as well as the occasional inclusion of elements such as spines, ribs and varices, contribute to the mollusc's structural ability to resist predators, but the way in which the calcium carbonate crystal building blocks are latticed together in different microstructures also plays a role (see Szabó 2008). Although *some* shell has the capacity to fracture conchoidally when force is applied in a particular way, fracture patterns largely diverge from those seen with stone. Thus, distinguishing human modification from the action of any number of taphonomic processes requires a thorough consideration of shell structure and resulting taphonomic and fracture proclivities as well as signatures of cultural and natural modification.

Although limpets are broadly similar in form, being ovoid in outline with a cap-shaped profile, the various limpet families are structurally very different (Fuchigami and Sasaki 2005; McClintock 1967; Nakano and Ozawa 2007). Investigation of the microstructural composition of *S. flexuosa* identified three distinct microstructural layers sandwiched together (Fuchigami and Sasaki 2005: 147); (1) an outer radial crossed lamellar layer, (2) a middle concentric crossed lamellar layer, and (3) an interior irregular complex cross foliated layer (see Figure 4). Crossed lamellar structures consist of aragonite (a form of $CaCO_3$) tablets or lamellae stacked together at three discrete levels of decreasing size. As explained by Fuchigami and Sasaki (2005: 155), the first order lamellae are arranged in radial or commarginal directions – in the case of limpets commarginal deposition is concentrically around the shell. The second-order lamellae are laid down as sheets, with each sheet alternating angle and growth direction. Third-order lamellae are deposited parallel to one another. Thus, the outer two layers of *S. flexuosa* shells are of the same structure, but differently aligned.

Patellid limpets are the only shells to generate a cross foliated structure in calcite (another form of $CaCO_3$) (Currey and Taylor 1974: 403; Wilmot et al. 1992: 21), and a complex version of this is seen in the innermost layer of *S. flexuosa*. Crossed foliated structures are very much like their counterpart in aragonite, the crossed lamellar structure (Fuchigami and Sasaki 2005: 161). In the irregular complex crossed foliated structure of the inner layer of *S. flexuosa*, the first-order lamellae are arranged patchily whilst the term 'complex' denotes that the folia are not arranged unidirectionally (Fuchigami and Sasaki 2005: 161). As noted by Currey and Taylor (1974: 403), the modulus of elasticity of this microstructure is high and the modulus of rupture remarkably so.

Although dominantly composed of $CaCO_3$, molluscan shells also have a proteinaceous component which acts as both a matrix for the crystals and decreases brittleness making the shells more resilient materials. Proteins enmesh the crystals within the structure with different microstructural types effecting this in different ways (Watabe 1988). Crossed structures typically have a very small protein fraction compared to other structures such as

nacre (mother-of-pearl) or the foliate structure of oysters (Dauphin and Denis 2000; Vermeij 1993: 47, 52). Although these proteins impart considerable strength to the overall shell material during the life of the mollusc, after death they are unable to be maintained and begin to deteriorate rapidly (Vermeij 1993: 50-51).

At a macro level shells are also designed to withstand external forces such as the actions of predators, desiccation and wave impact. *S. flexuosa*, like many other limpets, creates a 'homing scar' in the rock where the animal returns after grazing algae from the surrounding area (Iwasaki 1999; Lindberg 2007). Indeed, *S. flexuosa* is known to 'garden' the algae around the home scar, creating conditions for the growth of target algae species (Lindberg 2007). The home scar of *S. flexuosa* has also been noted to have a very particular morphology with the outer circumference of the scar precisely fitted to the crenelated margins of the shell, with an interior depression that matches the shape of the animal's foot (Lindberg 2007: 222). Unlike many other types of limpets and intertidal molluscs, this means that the margin of the shell is generally protected from predators and the elements and observation of the archaeological sample from Golo Cave does suggest that margin damage during life is rare. Juvenile *S. flexuosa* lack the distinctive crenelated margins (Lindberg 2007: 225) which further confirms that all of the *S. flexuosa* shells within the Golo Cave sample are mature.

Although *S. flexuosa* is considered a small species within the scutellastrid clade (Lindberg 2007), the shells are consistently larger than one of the other major species of limpet represented at Golo Cave, *Patelloida striata*, which has an average maximum body size of 24.3 mm (Kurihara 2002). The size of *Cellana radiata*, the dominant limpet species at Golo Cave, is variable dependent on position on the shore with an average maximum size of 31-33 mm being attained in the lower reaches of the intertidal, 22-24 mm in the middle intertidal and 16-18 mm in the highest intertidal areas (Balaparameswara Rao and Ganapati (1971: 111). The average size of modern *S. flexuosa* from Moorea, French Polynesia, was calculated to be 33 mm (Lindberg 2007: 228), however the average size of the *S. flexuosa* specimens obtained from the Philippines (Bohol) for the experimental portion of this study (n = 28) was 24.53 ± 3.51 mm. A further three species sourced from west Java were larger, with an average length of 42.37 ± 3.41 mm. Length measurements of the unbroken archaeological *S. flexuosa* shells were also taken (n = 37) and gave an average of 37.49 ± 8.89 mm.

Given their size and naturally-serrated edge, *S. flexuosa* utilised as a tool would seem hypothetically suited to a scraping or cutting function. The fact that the shells are designed to be strong in multiple directions, and withstand a range of diverse forces (Vermeij 1993: 70-72) also supports their potential suitability as expedient tools. The edge-rounding noted on several specimens during the course of midden analysis acted as a catalyst to further understand both the nature of natural fracture and the action of the taphonomic processes in *S. flexuosa* as well as initiating a series of experimental use-wear tests.

Methodology

To identify whether the *S. flexuosa* specimens with apparent edge-rounding were generated by natural or taphonomic processes, or through the deliberate use of the shells as expedient tools, the parameters of natural and cultural modifications to the shell margins needed to be defined. The aim was to test and generate comparative specimens reflecting processes that could cause fracture and attrition of the shell margins. Although many use-wear experiments seek to identify specific types of working and relate these to characteristic patterns of wear, this was not our aim here. The potential range of, especially cultural processes, is both diverse and largely unknown. Thus, we sought rather to investigate a range of material textures, as opposed to specific actions, to see if working these generated identifiable and characteristic differences in use-wear.

Prior to undertaking any testing or analysis, all experimental and archaeological *S. flexuosa* specimens underwent a taphonomic assessment. This assessment included detailing any chips or cracks present, or any bioerosion or adhesions that could influence results. Such features were only noted to a very minor degree on the specimens used for experimental work. The two major forms of taphonomic modification consistently noted were some erosion to the apex of the shell and the covering of the outer surface of the shell with coralline algae and relict adhering calcareous worm tubes, however both of these commonly occur during the life of the animal (Lindberg 2007; Smyth 1989). All experimental specimens were collected live and thus do not show the typical signatures of the post-mortem action of littoral taphonomic processes such as beachrolling (see Zuschin et al. 2003 for a discussion of a range of such processes). Additionally, all visible signs of burning to specimens were noted and did not include any of the potentially worked shells. X-ray diffraction analysis of both fresh and archaeological shells did not show evidence of recrystallization in the archaeological sample and no evidence of recrystallization/reprecipitation was noted under the microscope.

To investigate natural patterns of fracture, an INSTRON static materials testing machine was used. The INSTRON machine loads compressive force on materials in a specified direction and calculates the point of structural failure. Our interest was not so much in the mechanical strength of the shells (e.g. Currey and Taylor 1974) as these values are strongly influenced by taphonomic factors. Rather, we wished to replicate the application of force in different directions and scrutinise the fracture surfaces for diagnostic patterns of damage. Three modern specimens of *S. flexuosa* were tested in different directions: anterior-posterior, lateral margins and dorsal-ventral (see Figure 2 for shell parts and terms).

To generate comparative use-wear specimens worked on a range of material textures, a variety of materials/activities were chosen that reflected both activities and available resources on Gebe Island and surrounds. These materials, the nature of the working, and the durations of the experiments are outlined in Table 3. Taro (*Colocasia esculenta*) and yam (*Dioscorea* spp.) are widely gardened and consumed starch staples in the Island

Southeast Asia and Pacific regions. They both require peeling before cooking and this is especially important with taro as its flesh and skin contains needle-like irritant crystals of calcium oxalate (Kumoro et al. 2014). Coconut flesh is also widely used across the Asia-Pacific region and it is common for the flesh (endosperm) to be scraped out of the endocarp with a mollusc shell (KS pers. obs.). Bamboo (*Bambusa* spp.) is a diverse and extensively used resource across the Asia-Pacific. Sections of the culm are frequently split and sometimes stripped for the manufacture of various products (e.g. West and Louys 2007). There are several species of wild boar (*Sus* spp.) native to the Southeast Asian region, and the domestic *Sus scrofa* was widely translocated across the islands of the Asia-Pacific in the Holocene (Dobney et al. 2008). Gebe Island is depauperate in terms of native terrestrial fauna, however a range of medium-sized marsupials were translocated to the island during the Holocene and *S. scrofa* was introduced within the last 3500 years (Flannery et al. 1998). The textures of pig skin, pork meat and pig bone are all different, and thus experiments were undertaken separately for each of these zones. Finally, small patches of red pigment, potentially haematite or iron-rich clay/ochre, were noted on some of the stone tools from Golo Cave. Thus, the scraping of a nodule of haematite was included in the use-wear experiments.

Drawing together all of these materials, a range of textures is represented. Yam and taro skins are soft but fibrous, whilst coconut flesh is soft and non-fibrous with a high saturated fat content. Bamboo culms are hard and fibrous whereas the nodule of haematite used was simply hard (Moh's hardness 6.5). Pig skin, flesh and bone all have differing textures with the skin being elastic and non-fibrous, the flesh being relatively soft and the bones being hard and non-fibrous.

After the usewear experiments were conducted, all *S. flexuosa* specimens were analysed using a low power stereo microscope. Modifications were systematically recorded and those shells showing key modifications were then analysed using a scanning electron microscope. Specimens were not coated so as to remain analogous with non-coated archaeological specimens analysed. They were all thus analysed using a low voltage setting, either 4 or 15 kV. Key archaeological specimens with noted potential use-wear were also analysed using a low power stereo microscope followed by low voltage scanning electron microscopy. Due to the heritage values of the archaeological material, no coating of specimens was undertaken.

Results of analysis

Simulated natural fracture

The three *S. flexuosa* specimens fractured using the INSTRON static materials testing machine produced shells broken in a variety of ways, and a series of characteristic fracture surfaces Compressive force delivered to the apex of the shell (dorsal-ventral direction) produced a radial crack from the margin, but no fragmentation. The outline of the crack is

263 rough and zigzags between travelling in a radial direction and following the concentric path
264 of the microstructure around the shell (Figure 5a).

265 With another *S. flexuosa* shell, force was applied to the anterior and posterior margins
266 simultaneously. The shell did not fail completely, but rather a section of the anterior margin
267 came away along largely concentric lines. Analysis of this fracture surface revealed not only
268 the different fracture paths of the various sandwiched layers (Figure 5b), but also the
269 'tearing' of bundles of crystal lathes from the main structure through the organic matrix
270 (Figure 5c).

271 With the final *S. flexuosa* shell used in the simulated natural fracture experiments,
272 compressive force was applied to the opposing lateral margins. The shell failed completely
273 and fragmented into six separate pieces. Under magnification, the fractured edges shared
274 many features with those noted for the posterior-anterior compressed specimen. The
275 different layers of shell tended to fracture along different paths, resulting in an irregular
276 outline and profile (Figure 5d). Once again, bundles of crystals appeared 'torn' from the
277 main structure, and fractures and incipient fractures ran in multiple directions (Figure 5e).
278 This latter observation accords with what we know of the differently aligned sandwiched
279 microstructural layers (see discussion of microstructure above). As noted by Hedegaard et
280 al. (1997: 332) "[p]atellogastropod shells tend to break along contours parallel to first-order
281 elements of the shell microstructures…", however the orientation of the first-order
282 elements varies in each layer.

283 Experimental working

284 *Taro peeling*

285 As summarized in Table 3, four *S. flexuosa* specimens were used in the taro peeling
286 experiments. Two were used for 20 strokes along the length of the corm, and two were
287 used for 100 strokes. For each series of strokes, the direction of movement was consistently
288 away from the body and the other towards it. For all experiments the limpet was held in
289 the right hand at the apex from both the inner and outer surfaces and the posterior margin
290 was used to work the material (see Figure 6).

291 None of the specimens fractured or failed during the experiment. Observable modifications
292 on specimens used for 100 strokes include microchipping at the margin (Figure 7a) and the
293 removal through abrasion of the outermost layer of shell on the exterior surface (Figure 7b
294 and 7c). There was no evidence of edge-rounding of the utilised portion of the margin
295 however there was frequently polish (Figure 7d). Rather, these sections were more angular
296 and showed differential removal of shell layers than non-utilised sections. Specimens
297 utilised for only 20 strokes also showed the beginnings of these modifications (Figure 7b).

S. flexuosa shell proved to be an effective tool in the peeling of corms of taro. The exterior skin of the corm was easily removed using both directions of movement of the peeling action.

Yam peeling

As with the taro peeling experiment, four *S. flexuosa* specimens were used: two for twenty strokes and two for one hundred strokes. Each set of twenty or one hundred strokes was completed in an action either towards or away from the body. The shells were held in the same manner as for the taro peeling experiments.

The specimens used for the yam peeling experiments manifested less damage and modification than those used for taro peeling. This is potentially to do with the presence of abrasive needle-shaped calcium oxalate raphides in raw taro skin and flesh, which are absent from yams (see Crowther 2009, Englberger et al. 2009: 161). Low-level microchipping was observed at the margin of the working edge (Figure 8a). There was also some removal of the outer layer of shell on the exterior surface, particularly within the furrows between elevated sculptural ribs where the soft yam interior accumulated during working (Figure 8b). No particular zones of polish were observed on worked edges.

The effectiveness of *S. flexuosa* as a peeler was even more apparent in the peeling of tubers of yam compared the peeling of taro. The lack of the layered exterior skin seen in corms of taro resulted in a smooth, even surface of the yam for the shell margin to grip in to, and easily remove.

Coconut scraping

The soft flesh of a coconut was scooped out of the endosperm (coconut shell) in three different ways: scraping away from the body using the posterior margin of the shell, scraping towards the body using the posterior margin, and using the lateral margin in a more concentric fashion to scoop out the coconut flesh. Two shells were used for each direction; one for twenty strokes and one for one hundred. The shell was held in the same way as for the taro and yam experiments.

Noted modifications did not tend to be as extensive as those noted for taro peeling but were more extensive that those recorded for the peeling of yam. The most notable modification was a glossy sheen which coated the working edges and large portions of the exterior surface of the shell (Figure 9a). On shells used for 100 actions, this sheen was also accompanied by a muting of the external sculpture indicating gentle, sustained abrasion (Figure 9b). Microflaking and chipping was seen at the margins (Figure 9c) of all experimental working actions, but tended to be more prevalent in specimens used for the scooping motion (Figure 9d). Also noted on the specimens used for scooping were opaque patches at the extremities of the margin where internal shell layers had begun to pull apart under pressure, thus changing the refractory properties of the shell (Figure 9e).

Scraping of coconut using shell, while not as dramatic in its effectiveness compared to the yam and taro experiments, can still be considered successful. A fine pulp of the coconut flesh was generated with each scraping motion of the shell. Scooping of the coconut flesh using the shell resulted in a much larger quantity of coconut flesh being collected in a shorter period of time.

Bamboo scraping

Bamboo is widely used in a range of ways and functions in the Asia-Pacific region. To attempt to reflect this diversity in working a range of experiments were structured. Three *S. flexuosa* specimens were used to work dry bamboo culms. The anterior margins of two specimens were used in a scraping action; one of the outer culm surface and the other on the inner. The posterior margins of the same shells were then used for one hundred strokes. Unlike the taro, yam and coconut experiments, strokes here were back and forth meaning that twenty strokes in fact constituted forty individual motions. A further single *S. flexuosa* specimen was used to scrape the outer surface of a culm. It was intended to be used for forty strokes, but fractured into four fragments after thirty-two.

All of the specimens used for scraping dry bamboo showed variable evidence of edge faceting, attrition and sometimes rounding on the most exposed sections of the margin (Figure 10a). On two specimens there was evidence of incipient fatigue fracture concentric with the ventral margin (Figure 10b).

A further three *S. flexuosa* specimens were used in the same scraping manner on bamboo culms which had been soaked in water for several days. Each specimen was used for either twenty, forty or one hundred back-and-forth strokes with the posterior margin being used on the outer surface of the culm and the anterior margin on the inner culm surface. None of the specimens fractured during use. There was very little observable modification with wet bamboo scraping. In specimens used for 100 strokes, microchipping and shell removal at the margin (Figure 10c), as well as some muting of external sculpture, was observed (Figure 10d).

Overall, the general lack of shell modification in the bamboo scraping experiments was surprising. Additionally, the shell did little to modify the bamboo culms whether soaked or dry.

Haematite scraping

Two specimens of *S. flexuosa* were used in an attempt to scrape fragments of red pigment from a nodule of haematite. The haematite nodule had been sawn in half with a diamond blade to provide a flat face for working. It was expected that the shell would be unable to produce powdered pigment through scraping and that the shell would quickly fracture working such a hard material. One shell was used to scrape the nodule face twenty times and the other was intended to be used for one hundred strokes. The specimen used for

twenty strokes showed distinct faceting along the most exposed sections of the posterior margin as well as bearing traces of bright red haematite powder (Figure 11a and 11b). As well as this residue adhering to the shell, a small quantity of loose powdered haematite was also generated. The specimen intended for one hundred strokes broke in two after fourteen strokes. However even at this point the working edge showed evidence of faceting and powdered haematite was also generated.

Pig skin, flesh and bone working

Six *S. flexuosa* specimens were used for working a leg of pig. Two shells were used to cut through the pig skin, two for cutting pork flesh and two for scraping flesh from the bone. Each activity was undertaken for twenty and then one hundred strokes with two different shells. None of the shells fractured during experimentation.

S. flexuosa was able to penetrate the skin of the pig, but not with less than twenty strokes. The shell specimen used for one hundred strokes yielded relatively widespread and varied patterns of modification when compared with the other experiments. The flaking away of sections of the outer most layers of the exterior shell surface is apparent across the working edge (Figure 12a). When viewed from the interior of the shell, this delamination of shell layers results in the margin appearing translucent and glassy (Figure 12b).

When compared with the cutting of pig skin, the damage observed from the cutting of pig flesh followed the same general trends, but modifications were more extensive. The delamination of the exterior most shell layers at the margin is more dramatic, with the natural crenelated outline eliminated (Figure 12c). Rather than creating a facet as seen in the processing of hard materials such as haematite, individual shell layers have split and splintered leaving a ragged, translucent zone even larger than that seen in the pig skin cutting experiment. In a similar process of attrition, the exterior sculpture has been muted as small flakes of shell along the ribs were removed (Figure 12c).

The series of protruding ribs along the margin of *S. flexuosa* shell acted as serrations to tear rather than cut through the pig flesh. While the pig flesh was able to be processed using the shell, the results were untidy.

The scraping of bone yielded remarkably different patterns of modification that seems largely attributable to the difference in texture. Unlike the elastic nature of skin, and even moreso the flesh, the bone presented a harder and less malleable substrate. Although facets have not been generated, the translucent lamellar edges are no longer present. Instead, edges are straight and more regular (Figure 12d). Repeated zones of contact have produced flattened sections of margin clearly visible in outline. In addition, shell material in a band directly back from the margin has been smoothed and abraded (Figure 12d). This smoothing is similar to that seen in pig flesh cutting, and is most likely caused by the contact of the shell on flesh and muscle adhering to the bone.

The defleshing of pig bone proved effective using the shell in a scraping motion across the surface of the bone. Little damage to the bone itself was observed once the majority of the adhering pig flesh was scraped away.

Analysis of archaeological *S. flexuosa* shells

Seventy-nine *S. flexuosa* shells and detached margin fragments were analysed using a low power digital microscope with some specimens being further examined using scanning electron microscopy. Most shells and shell fragments did not show signs of modification consistent with the use-wear patterns generated in the experimental working phase. Most *S. flexuosa* margins had damage at some point around the perimeter, however these most often matched the bending fractures seen in the INSTRON-fractured specimens and thus indicated natural or taphonomic fracture (e.g. trampling). Despite this conclusion, the level of modification seen in the experimental working of soft materials such as taro and yam was slight, and hence theoretically difficult to detect in archaeological specimens where minor taphonomic damage to shell margins is frequent.

Five shells were identified as have clearly non-natural modifications. There are two major and discrete identifiable wear patterns: edge-rounding and/or faceting at the margin, and abrasion of the elevated sculpture on either the posterior or anterior outer shell surface. Both patterns of modification have analogues to some degree with the experimentally-worked *S. flexuosa* shells, and both are very distinct from each other.

Three partial *S. flexuosa* shells showed evidence of edge-rounding and faceting at the break surface. One was recovered from Square M4: 185-190cm depth, and a further two from 200-205cm depth in the same square. Chronologically, these shells are associated with two radiocarbon dates from between 190cm and 205cm in square M4: 29,355 – 31,495 cal. BP (2 sigma) and 32,167 – 32,919 cal. BP. The *S. flexuosa* from 185-190cm (accession code: PafGC023) and one of the shells from 200-205cm depth (accession code: PafGC063), show planes of abrasion along the break surfaces at the posterior shell margin (Figure 13a and 13b). This abrasion has evenly reduced the different layers of shell leaving a smooth and regular edge (Figure 13c and 13d). Under magnification, flat, even facets can be seen where the edges contacted the material being worked, and this is especially noticeable in PafGC063 (Figure 13b). The only experimentally-worked *S. flexuosa* shells to show the generation of flat facets were those used to scrape haematite. A hard material is required to create regular, flattened surfaces on the shell margins and this suggests that the two *S. flexuosa* shells from Golo Cave showing this pattern were utilised in the worked of a hard substance. This interpretation is further supported by the noting of attritional wear on the most elevated parts of the shell sculpture near the edge on both specimens, but no modification to the furrow surfaces between the radial ribs (Figure 13a).

The remaining *S. flexuosa* recovered from 200-205cm depth shows a contrasting pattern of edge rounding and anterior margin modification. Instead of flattened facets and a

regularised edge, specimen PafGC008 has rounded edges on a more irregularly-shaped margin and a distinctive zone of flakey shell removal in a band back from the working edge (Figure 13e). This particular type of modification closely matches that seen in the experimental scraping of pig bone. In that instance, the wear pattern was produced through contact with a combination of hard and soft, elastic substrates. The same combination of the working of hard and soft materials, either simultaneously as with the scraping of bone, or as separate events, has most likely generated the transformations noted in PafGC008.

Two further partial shells showed a different pattern of modification. Specimen PafGC015 was recovered from 200-205cm depth in Square M4, and PafGC041 was identified from within the midden assemblage from 205-210cm depth in the same square. Rather than modification of the edge of the shell, these two specimens show localised abrasion on the dorsal, or outer, shell surface. For PafGC015, the major posterior radial rib has been smoothed whilst adjacent surfaces retain their rough, natural sculpture (Figure 14a). For PafGC041, a major anterior rib shows similar wear from the apex of the shell to the margin (Figure 14b).

None of the experimentally-worked *S. flexuosa* match the wear pattern seen in these two specimens, however smoothing and the muting of sculpture was seen in a more extensive manner with the scooping of coconut. Given that only the most elevated portions of the sculpture have been affected in the Golo Cave examples, we can surmise that a less malleable material was being worked which left the interstices between the ribs untouched during the working process. The restriction of the wear to a single rib indicates that a much smaller section of the shell was in contact with the material being worked. This restrictiveness also indicates that less discriminate taphonomic processes, such as weathering or attrition through movement, were not responsible for the patterns of modification observed here. Sculptural muting generated by taphonomic processes either within a site or a natural littoral setting will occur over the entire surface of the shell (e.g. see Zuschin et al. 2003), and very specific processes are required to produce such localised modifications.

The five different *S. flexuosa* shells from Golo Cave identified as having been worked show three different patterns of modification. Two show edge faceting and rounding congruent with the working of a hard material. One shows edge rounding and the removal of shell material near the margin that most closely accords with the working of a combination of hard and soft, elastic materials such as seen in the experimental scraping of fresh pig bone. The final class of modification, noted in two specimens, has no clear analogue within the experimental sample. These specimens show a very localised patch of smoothing and wear on the dorsal surface of the shell. However this wear is restricted to only the most elevated portions thus suggesting the focused working of a rigid material. None of these modifications bear any similarity to recorded natural or taphonomic modifications.

Limpet scrapers in the context of early Southeast Asian shell artefact use

The analysis of natural fracture patterns in *S. flexuosa*, as well as wear and damage patterns generated by a range of generic cultural actions, demonstrates that the five shells isolated were most likely modified through human action. All areas exhibiting traces of use-wear are discrete, with other zones of each shell retaining their natural sculpture and morphology. Three different types of use-wear were recorded, and the experimental work suggests that different media were being worked and different actions used to generate this diversity.

Unlike the large *Turbo marmoratus* shells, gathered from subtidal waters with a vision to produce artefacts, and the fragments of *Nautilus* sp. which – by virtue of their deep-sea ecology – could not have represented a food source (Szabó et al. 2007), *S. flexuosa* are a key subsistence species in the Pleistocene shell midden at Golo Cave. The character of the shell midden and range of species present suggests that *S. flexuosa* shellfish would have been available in close proximity to the site, and were collected with a range of other intertidal limpets and other molluscs for consumption. The majority of *S. flexuosa* shells show no signs of use as tools, although their size and sharp, crenulated margins would have made for a convenient and effective multipurpose tool. The working experiments demonstrate their efficacy with a range of simple tasks.

Unlike the *Callista chione* and *Glycymeris* sp. shells of Mousterian sites (Douka and Spinapolice 2012: 73) the margins of *S. flexuosa* are not dull and thus do not require deliberate retouching to function as an effective edge-tool. Neither is there evidence for the post-mortem collection of *S. flexuosa* for explicit use as a raw material (see Douka and Spinapolice 2012: 58). Rather, some of the Golo Cave *S. flexuosa* shell were 'repurposed' for use as tools, and the dual examples of two different wear patterns observed indicate that this repurposing was perhaps not entirely random. Although the present sample is too small to make a strong case, it seems possible that *S. flexuosa* shells were seen as appropriate for particular tasks and were regularly selected to undertake these.

Taken together, the *T. marmoratus* operculum and *S. flexuosa* limpet data show that shell was a key raw material for the Pleistocene occupants of Golo Cave. Work continues on the analysis of the associated reduced *T. marmoratus* shells, which appear to have been delicately chipped back in a standardised way, and fragments of the pelagic *Nautilus* cf. *pompilius*, which seem to have been cut into small tabs. These shell technologies are diverse in the raw materials employed, the collection strategies enacted to procure them, the methods by which they were used and modified, and doubtless the uses to which they were put. While on some level it may be true that shell filled a technological void left by the local absence of quality lithic resources (Douka and Spinapolice 2012: 69), this situation apparently fostered the development and diversification of shell technologies. Contrasted against the simple and loosely-structured lithic assemblage from Golo Cave (see Szabó et al. 2007), shells were collected, repurposed, modified and used in a set of diverse and highly-structured ways.

At present, the methodological cupboard is relatively bare when it comes to the recognition and interpretation of minimally-modified and utilised but non-modified shell. While taking cues from the technological analysis of lithic artefacts can provide useful directions, the status of shell as a biomaterial specifically generated to withstand environmental pressures (Vermeij 1993) means that the two categories of material are not equivalent. To complicate matters further, the structure, composition and mechanical properties of different families of shell are very varied, meaning that conclusions regarding one type of shell cannot be readily applied to another. With this in mind, it is possible that the other major species of limpet (*Cellana radiata*) represented in the Pleistocene deposits at Golo Cave was also occasionally used as a tool, but a separate programme of analysis would be required to investigate this.

Acknowledgements

This work was undertaken with funding provided by the Australian Research Council in the form of a QEII fellowship and Discovery Grant (DP0987164) awarded to Szabó. Firstly, thank you to Peter Bellwood for his ongoing support of the analysis of the Golo Cave shell. Newly presented radiocarbon determinations were kindly produced courtesy of John Dodson of the Australian Nuclear Science and Technology Organisation. We would like to thank Hugh Brown, Zhixin Chen and Nick Mackie of the University of Wollongong, Faculty of Engineering for access to facilities and guidance on experimental possibilities and procedures. Thanks also to José Abrantes and Brian Jones of the School of Earth and Environmental Sciences for XRD assistance and Penny Williamson for help in sourcing samples for the experimental work.

References

Balaparameswara Rao, M. and P.N. Ganapati. 1971. Ecological studies on a tropical limpet *Cellana radiata*. *Marine Biology* 9: 109-114.

Bellwood, P., G. Nitihaminoto, G. Irwin, Gunadi, A. Waluyo, and D. Tanudirjo. 1998. 35,000 years of prehistory in the Northern Moluccas. In *Bird's head approaches: Irian Jaya studies, a programme for interdisciplinary research*, ed. G. Bartstra, 233–75. Rotterdam and Brookfield: A. A. Balkema.

Choi, K. and D. Driwantoro. 2007. Shell tool use by early members of *Homo erectus* in Sangiran, central Java, Indonesia: cut mark evidence. *Journal of Archaeological Science* 34: 48-58.

Crowther, A. 2009. Reviewing raphides: issues with the identification and interpretation of calcium oxalate crystals in microfossil assemblages. In Fairbairn, A., O'Connor, S. and

564 Marwick, B. (eds) *New Directions in Archaeological Science*. Terra Australis 28, pp 105-118,
565 Canberra: ANU E-Press.
566
567 Currey, J.D. and J.D. Taylor. 1974. The mechanical behaviour of some molluscan hard
568 tissues. *Journal of the Zoological Society, London* 173:395-406.
569
570 Dauphin, Y. and A. Denis. 2000. Structure and composition of the aragonitic crossed lamellar
571 layers in six species of Bivalvia and Gastropoda. *Comparative Biochemistry and Physiology*
572 *Part A* 126: 367-377.
573
574 Dobney, K., T. Cucchi, and G. Larson. 2008. The Pigs of Island Southeast Asia and the Pacific:
575 New Evidence for Taxonomic Status and Human-Mediated Dispersal. *Asian Perspectives* 47
576 (1): 59-74.
577
578 Douka, K. and E.E. Spinapolice. 2012. Neanderthal Shell Tool Production: Evidence from
579 Middle Palaeolithic Italy and Greece. *Journal of World Prehistory* 25:45-79.
580
581 Englberger, L., K. Albert, A. Lorens and A. Levendusky. 2009. Taro: An important Pohnpei
582 staple food. In M.J. Balick (ed.) *Ethnobotany of Pohnpei* pp. 132-164. Honolulu: University of
583 Hawai'i Press.
584
585 Flannery, T. F., P. Bellwood, J. P. White, T. Ennis, G. Irwin, K. Schubert, and S.
586 Balasubramaniam. 1998. Mammals from Holocene archaeological deposits on Gebe and
587 Morotai Islands, Northern Moluccas, Indonesia. *Australian Mammalogy* 20:391–400.
588
589 Fuchigami, T. and T. Sasaki. 2005. The shell structure of the Recent Patellogastropoda
590 (Mollusca: Gastropoda). *Paleontological Research* 9(2):143-168.
591
592 Irwin, G., P. Bellwood, G. Nitihaminoto, D. Tanudirjo, and L. Siswanto. 1999. Prehistoric
593 relations between Island Southeast Asia and Oceania: Recent archaeological investigations
594 in the Northern Moluccas. In J.C. Galipaud and I. Lilley (eds) *The Pacific from 5000 to 2000*
595 *BP: Colonisation and transformations*, pp. 363–74. Paris: Institut de Recherche pour le
596 Développement.
597
598 Iwasaki, K. 1999. Short- and long-term movements of the patellid limpet *Patella flexuosa*
599 within gaps in intertidal mussel beds. *Journal of Molluscan Studies* 65: 295-301.
600
601 Kumoro, A.C., Rr.D.A. Putri, C. S. Budiyanti, D. S. Retnowati and Ratnawati. 2014. Kinetics of
602 Calcium Oxalate Reduction in Taro (*Colocasia esculenta*) Corm Chips during Treatments
603 Using Baking Soda Solution. *Procedia Chemistry* 9: 102-112.
604
605 Kurihara, T. 2002. Spatial and temporal fluctuation in the density of the intertidal limpet,
606 *Patelloida striata* Quoy and Gaimard, on subtropical cobbled shores. *Journal of Molluscan*
607 *Studies* 68: 79-86.
608

Nakano, T. and T. Ozawa. 2007. Worldwide phylogeography and limpets of the Order Patellogastropoda: molecular, morphological and palaeontological evidence. *Journal of Molluscan Studies* 73: 79-99.

Pasveer, J. M., and P. Bellwood. 2004. Prehistoric bone artefacts from the Northern Moluccas, Indonesia. In S. G. Keates and J. M. Pasveer (eds) *Modern Quaternary research in Indonesia*, pp. 301–59. Lisse: A. A. Balkema.

Smyth, M.J. 1989. Bioerosion of gastropod shells: with emphasis on effects of coralline algae cover and shell microstructure. *Coral Reefs* 8:119-125.

Stuiver, M., and P.J. Reimer. 1993. Extended 14C database and revised CALIB radiocarbon calibration program. *Radiocarb.* 35:215-230

Szabó, K. 2008. Shell as a raw material: mechanical properties and working techniques in the tropical Indo-West Pacific. *Archaeofauna* 17:125-138.

Szabó, K. 2013. Identifying worked shell: a consideration of methodological issues of particular relevance to Pleistocene contexts. In G. Bailey, K. Hardy and A. Camara (eds) *Shell Energy: Prehistoric Coastal Resource Strategies*, pp. 277-286. Oxford: Oxbow.

Szabó, K., A. Brumm and P. Bellwood. 2007. Shell artefact production at 32,000 – 28,000 BP in Island Southeast Asia: thinking across media? *Current Anthropology* 48:701-723.

Vermeij, G. J. 1993. *A Natural History of Shells.* Princeton, Princeton University Press.

Watabe, N. 1988. Shell Structure. In E.R. Trueman and M.R. Clarke (eds) *Form and Function: The Mollusca, volume 11*, pp. 69-104. San Diego and London: Academic Press.

West, J.A. and J. Louys. 2007. Differentiating bamboo from stone tool cutmarks in the zooarchaeological record with a discussion on the use of bamboo knives. *Journal of Archaeological Science* 34: 512-518.

Wilmot, N.V., D. J. Barber, J.D. Taylor and A.L. Graham. 1992. Electron Microscopy of Molluscan Crossed-Lamellar Microstructure. *Philosophical Transactions: Biological Sciences* 337(1279):21-35.

Zuschin, M., M. Stachowitsch and R.J. Stanton Jr. 2003. Patterns and processes of shell fragmentation in modern and ancient environments. *Earth-Science Reviews* 63: 33-82.

Figure 1: Map showing the location of Gebe Island and Golo Cave.

Figure 2: Archaeological *Scutellastra flexuosa* from Golo Cave showing dorsal, lateral and ventral views.

Figure 3: Golo Cave *Scutellastra flexuosa* with putative working noted during the original shell midden analysis. From Square M4, 200-205cm depth.

Figure 4: Schematic illustrations of crossed structures present in *S. flexuosa*. A: crossed lamellar structure; (1) inner surface (2) commarginal section (3) radial section (4) oblique three dimensional view. B: Irregular complex crossed foliated structure; (1) inner surface (2) commarginal section (3) radial section (4) oblique three dimensional view. Redrawn from Fuchigami and Sasaki (2005: figure 16).

Figure 5:

S. flexuosa used for simulated natural fracture experiments: (a) irregular crack radiating from the margin to the apex. Concentric fatigue fractures are also visible, 40x magnification; (b) Various diverse fracture paths of stacked layers in anterior-posterior compressive force delivery, 160x magnification; (c) Scanning electron microscope image of a fracture edge showing 'tearing' apart of bundles of crystals; (d) Various diverse fracture paths of stacked layers in lateral compressive force delivery, 40x magnification; (e) Fracture edge showing 'tearing' apart of bundles of crystals as well as multidirectional fracture paths, 80x.

Figure 6: Photo showing the way in which the *S. flexuosa* shells were gripped during working experiments – in this instance for the peeling of a taro corm.

Figure 7:

S. flexuosa used for taro peeling experiments: (a) microchipping at posterior margin, taro peeling 100x away from body, 65x magnification; (b) the removal of shell from the exterior surface of the posterior margin, taro peeling 20x away from body, 40x magnification; (c) Scanning Electron Microscope image of shell removal at the exterior posterior margin, taro peeling 20x away from body; (d) microchipping and polish at the posterior margin, taro peeling 100x away from body, 45x magnification.

Figure 8:

S. flexuosa used for yam peeling experiments: (a) microchipping at posterior margin, yam peeling 100x away from body, 45x magnification; (b) removal of portions of outer layer of shell in furrows between ribs on exterior, yam peeling 100x away from body, 55x magnification.

Figure 9:

S. flexuosa used for coconut flesh scraping: (a) glossy sheen across exterior surface, coconut scooping 100x, 40x magnification; (b) muting of exterior surface sculpture, coconut scooping 100x, 40x magnification; (c) chipping at margin, coconut scraping 100x away from body, 40x magnification; (d) microchipping at margin, coconut scooping 100x, 50x magnification; (e)

opaque patches at margin as a result of pressure exerted on the shell's edge, coconut scooping 100x, 50x magnification.

Figure 10:

S. flexuosa used for scraping the interior and exterior of soaked and dry bamboo culms: (a) faceting and residue at margin, dry bamboo exterior scraping 100x, 45x magnification; (b) concentric fatigue fractures visible on interior shell surface, dry bamboo exterior scraping 100x, 20x magnification; (c) microchipping at margin, soaked bamboo interior of culm 100x, 80x magnification; (d) muting of exterior surface sculpture, soaked bamboo exterior of culm 100x, 50x magnification.

Figure 11:

S. flexuosa used for scraping a nodule of haematite: (a) faceting and accumulation of residue at margin, haematite scraping 20x, 45x magnification; (b) Scanning Electron Microscope image of facet and adhering residue, haematite scraping 20x. The small highly reflective particles on the surface are fragments of powdered haematite.

Figure 12:

S. flexuosa used for cutting pig skin: (a) flaking of exterior shell layers, pig skin cutting 100x, 50x magnification; (b) translucence at margin from material lost on outer surface, pig skin cutting 100x, 55x magnification. *S. flexuosa* used for cutting pig flesh: (c) flaking and splintering of shell at margin resulting in translucence. Also loss of sculpture on body surface, 55x magnification. *S. flexuosa* used for scraping pig bone: (a) margin attrition and zone of exterior smoothing, pig bone scraping 100x, 30x magnification.

Figure 13:

S. flexuosa shells from Golo Cave with edge-rounding and faceting: (a) Specimen PafGC023, from Square M4 185-190cm depth. Rounding and faceting of fractured shell posterior with attritional wear on elevated sculpture but not in intervening furrows, 50x magnification; (b) Specimen PafGC063, from Square M4 200-205cm. Rounding and faceting of fractured shell posterior edge, 40x magnification; (c) Scanning Electron Microscope image of PafGC063 worked edge showing even shell removal and lack of chipping, tearing of differential wear across layers; (d) Scanning Electron Microscope image of PafGC063 showing the different orientations of shell within the fracture edge cross-section and the even removal of each through abrasion; (e) Specimen PafGC008, from Square M4 200-205cm depth. Rounding across edge with irregular outline and removal of shell material in a band back from the working edge, 40x magnification.

Figure 14

715 *S. flexuosa* shells from Golo Cave with abrasion to localised patches on the dorsal surface:
716 (a) Specimen PafGC015, from Square M4 200-205cm depth. Abrasion and muting of
717 sculpture of the main elevated posterior rib, 15x magnification; (b) Specimen PafGC041,
718 from Square M4 205-210cm depth. Abrasion and muting of sculpture on one of the main
719 anterior radial ribs, 20x magnification.

720

721

722 Table 1: Radiocarbon results by square and depth. Recalibrated from Bellwood et al. (1998)
723 with the addition of recently acquired determinations. Calibrated using Calib 7.0.2 with the
724 Marine13 calibration data set for shell and the IntCal13 data set for charcoal (Stuiver and
725 Reimer 1993). A ΔR value of 0 has been used for shell samples as has been recommended
726 for this region (F. Petchey, personal communication, 2007).

727 Table 2: Pleistocene shell midden species list and MNI data for Square M4, 175-250 cm
728 depth range. A further forty-eight taxa from this square and depth range were identified
729 where MNI equals less than five. *Denotes landsnail species.

730 Table 3: Table outlining the experimental materials, actions and durations.

731

Table

Lab code	Material	Square and depth	^{14}C age BP	1 sigma	2 sigma
ANU-9449	Marine shell	M4 (50-55 cm)	7400±10	5895 – 5955	5866-5976
OZN896 (AMS)	Balanid barnacle side plate - unburnt	M4 (170-175 cm)	29390±190	31004 - 3519	30718 - 31725
OZN895 (AMS)	*Barbatia amygdalumtostum*	M4 (190-195 cm)	30960±190	32365 - 32754	32167 - 32919
Wk-17764 (AMS)	*Drupa clathrata*	M4 (200-205 cm)	28740±474	29664 - 30885	29355 - 31495
ANU-9448	Charcoal	M5 (45-55 cm)	3230±80	1574 - 1610 (19 %) 1431 - 1565 (81 %)	1372 - 1691 (95 %) 1301 - 1357 (5 %)
OZN893 (AMS)	*Turbo setosus* operculum - unburnt	M5 (95-100 cm)	10210±60	9190 - 9308	9117 - 9407
OZN894 (AMS)	*Turbo setosus* operculum - unburnt	M5 (125-130 cm)	11440±60	10854 - 11041	10787 - 11135
ANU-9769	Marine shell	M5 (135-140 cm)	10540±70	9671 - 10026	9428 - 10092
ANU-9512	Marine shell	M5 (145-150 cm)	11480±70	10913 - 11115	10807 - 11180
ANU - 11053	Marine shell	M5 (195-200 cm)	19080±140	20445 - 20743	20329 - 20967
ANU-9768	Marine shell	M5 (195-200 cm)	9260±80	8041 – 8232 (89 %) 8006 – 8036 (11%)	7844 - 8292
ANU-9447	*Turbo* sp. operculum	M5 (230-235 cm)	31030±400	32243 - 32954	31938 - 33384
ANU-11007	Marine shell	LM6 (205-210 cm)	21780±160	23612 - 23909	23396 - 24028
Wk-17762 (AMS)	*Turbo marmoratus* operculum - retouched	LM6 (205-210cm)	16236±101	16999 - 17262	16912 - 17449
Wk-17761 (AMS)	*Turbo marmoratus* operculum - unretouched	LM6 (210-215 cm)	28251±305	29315 - 30020	29185 - 30606
Wk-4629	*Turbo marmoratus* operculum	LM6 (210-215 cm)	32210±320	33408 - 34115	33042 - 34375

Table

Species	MNI
Cellana radiata	397
Patelloida striata	205
Nerita costata	105
Scutellastra flexuosa	77
**Planispira* sp.	56
**Videna/Trochomorpha* sp.	16
Thais aculeata	16
Nerita polita	14
**Naninia* sp.	12
Purpura panama	10
Turbo spp. operculum	7
Reishia cf. *bitubercularis*	5

Table

Accession Number	Experiment	Identified texture	Action	Direction of movement	Number of movements
Paf001	Taro	Soft and fibrous	Peeling	Towards body	20
Paf002	Taro	Soft and fibrous	Peeling	Towards body	100
Paf003	Taro	Soft and fibrous	Peeling	Away from body	20
Paf004	Taro	Soft and fibrous	Peeling	Away from body	100
Paf005	Coconut	Soft, not fibrous	Scraping	Towards body	20
Paf006	Coconut	Soft, not fibrous	Scraping	Towards body	100
Paf007	Coconut	Soft, not fibrous	Scraping	Away from body	20[a]
Paf008	Coconut	Soft, not fibrous	Scraping	Away from body	100
Paf009	Coconut	Soft, not fibrous	Scooping	-	20
Paf010	Coconut	Soft, not fibrous	Scooping	-	100
Paf011	Pig skin	Soft, elastic	Cutting	-	20
Paf012	Pig skin	Soft, elastic	Cutting	-	100
Paf013	Pig flesh	Soft, elastic	Cutting	-	20
Paf014	Pig flesh	Soft, elastic	Cutting	-	100
Paf015	Pig bone	Hard, not fibrous	Scraping	Back-and-forth	20
Paf016	Pig bone	Hard, not fibrous	Scraping	Back-and-forth	100
Paf017	Yam	Soft and fibrous	Peeling	Towards body	20
Paf018	Yam	Soft and fibrous	Peeling	Towards body	100
Paf019	Yam	Soft and fibrous	Peeling	Away from body	20
Paf020	Yam	Soft and fibrous	Peeling	Away from body	100
Paf021	Dry bamboo	Hard and fibrous	Rubbing	Back-and-forth	20[b]/100[c]
Paf022	Dry bamboo	Hard and fibrous	Rubbing	Back-and-forth	40[d]
Paf028	Dry bamboo	Hard, fibrous	Rubbing	Back-and-forth	20[i]/100[j]
Paf023	Soaked bamboo	Hard and fibrous	Rubbing	Back-and-forth	20[e]
Paf024	Soaked bamboo	Hard and fibrous	Rubbing	Back-and-forth	40[f]
Paf025	Soaked bamboo	Hard and fibrous	Rubbing	Back-and-forth	100[g]
Paf026	Haematite	Hard, not fibrous	Scraping	Back-and-forth	20
Paf027	Haematite	Hard, not fibrous	Scraping	Back-and-forth	100[h]
Paf029	INSTRON	-	-	Dorsal-Ventral	-
Paf030	INSTRON	-	-	Anterior-Posterior	-
Paf031	INSTRON	-	-	Lateral	-

a) Fractured into two fragments after five strokes
b) Posterior margin of Paf021 used for twenty strokes
c) Anterior margin of Paf021 used for one hundred strokes
d) Fractured into four fragments after thirty two strokes
e) Anterior margin of Paf023 used for rubbing exterior of bamboo culm, and posterior margin used for rubbing interior of bamboo culm
f) Anterior margin of Paf024 used for rubbing exterior of bamboo culm, and posterior margin used for rubbing interior of bamboo culm
g) Anterior margin of Paf025 used for rubbing exterior of bamboo culm, and posterior margin used for rubbing interior of bamboo culm
h) Fractured into two fragments after fourteen strokes
i) Posterior margin of Paf028 used for twenty strokes
j) Anterior margin of Paf028 used for one hundred strokes

Figure

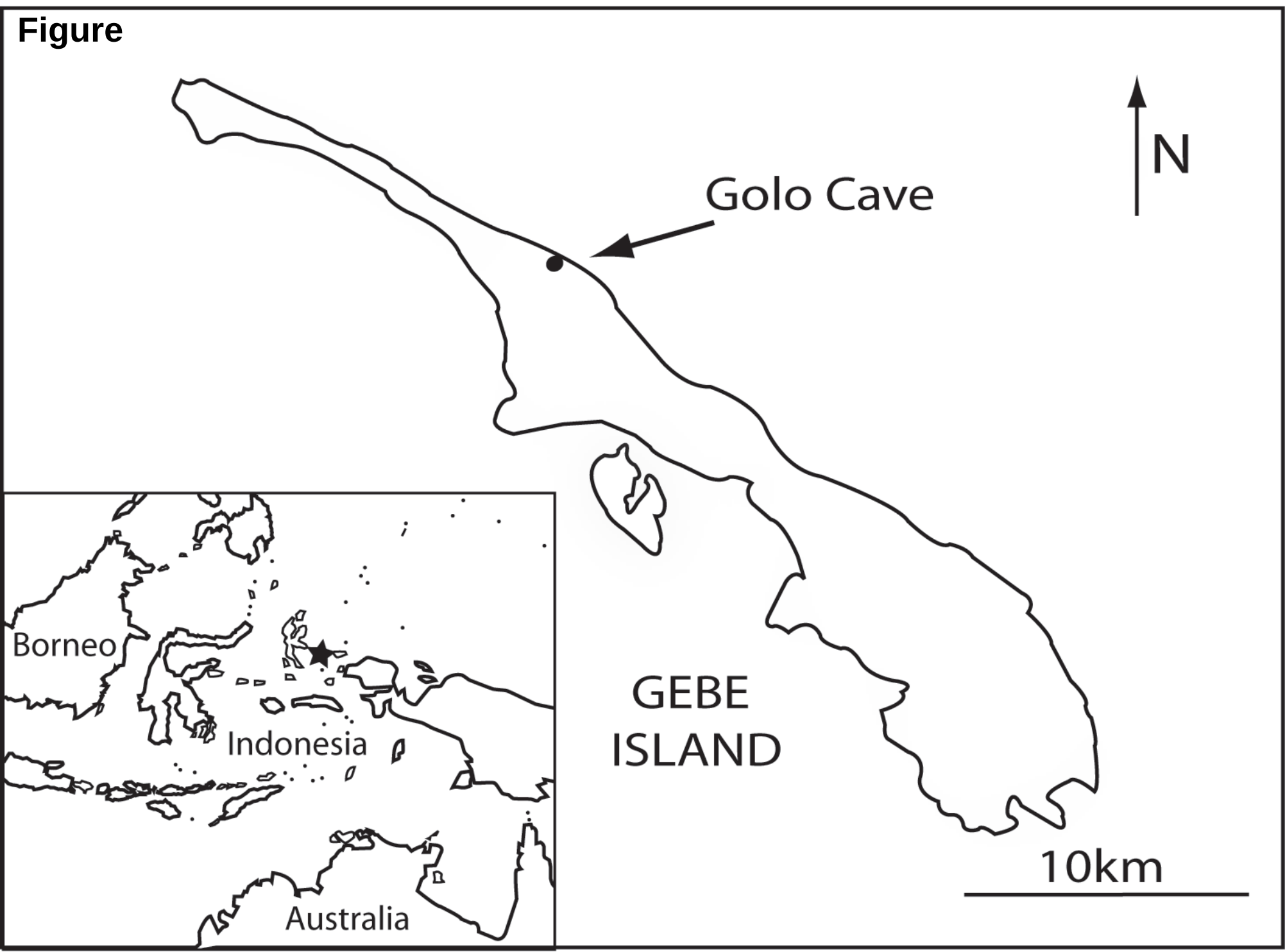

Figure
Click here to download high resolution image

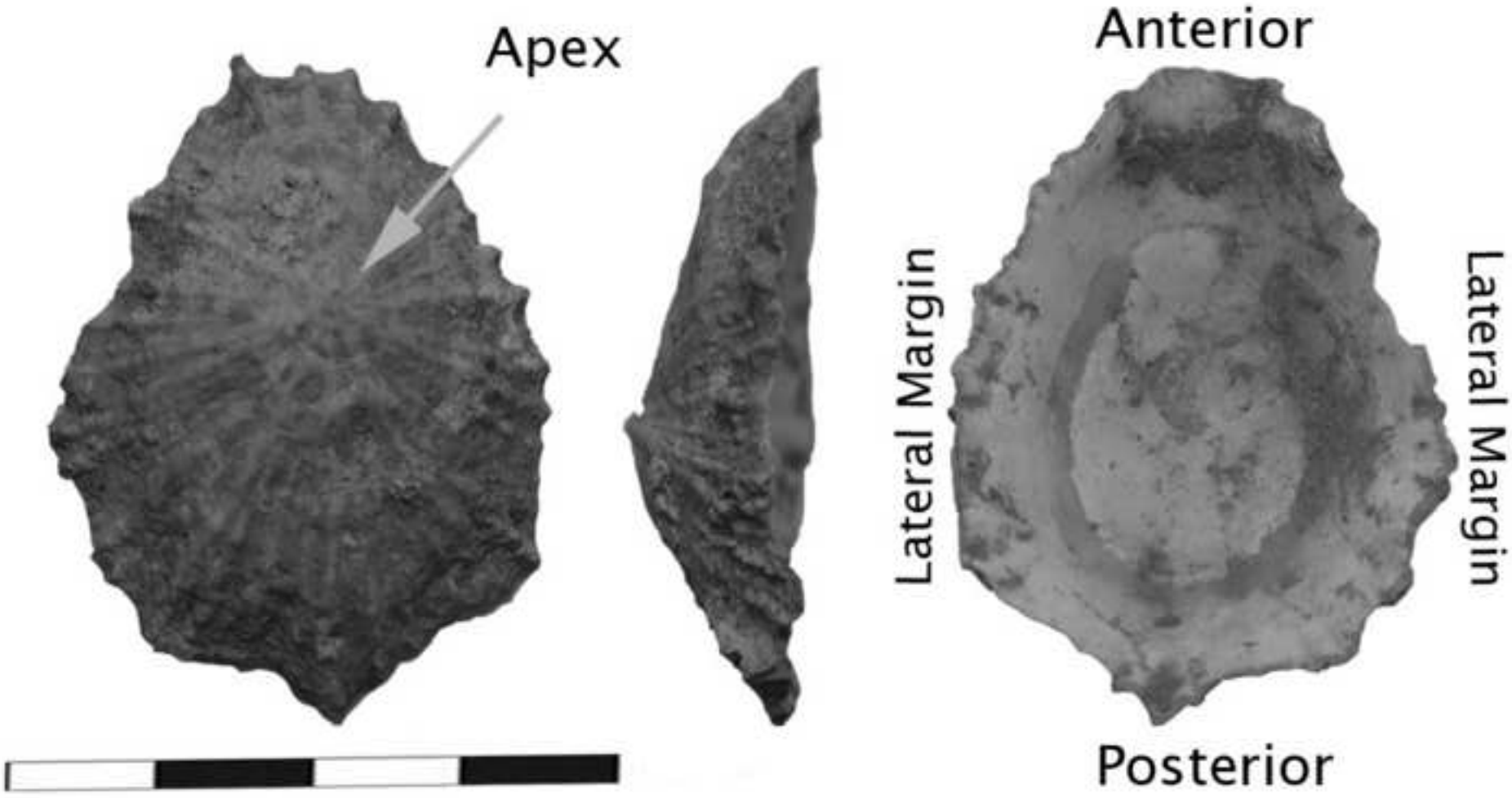

Figure

Click here to download high resolution image

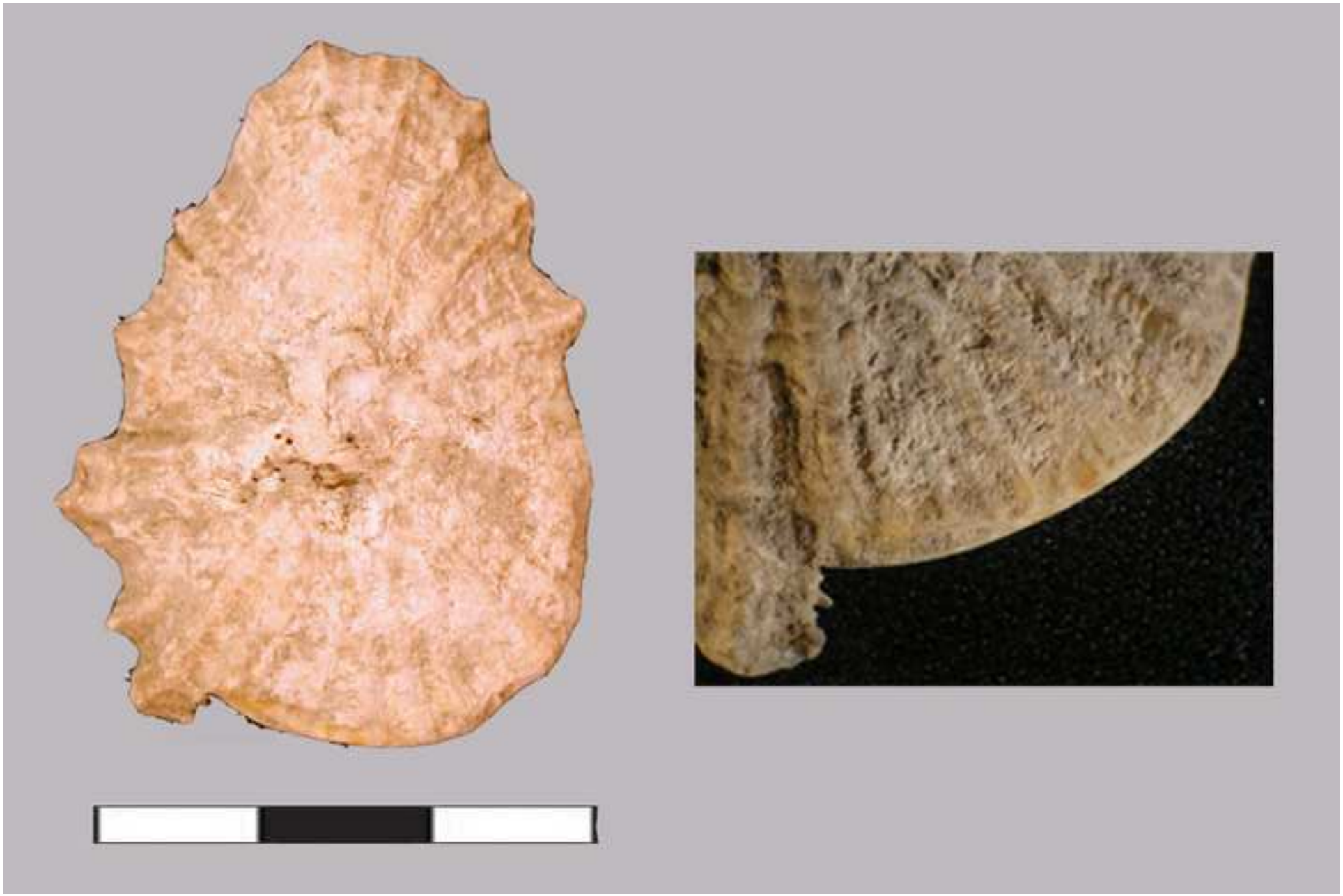

Figure

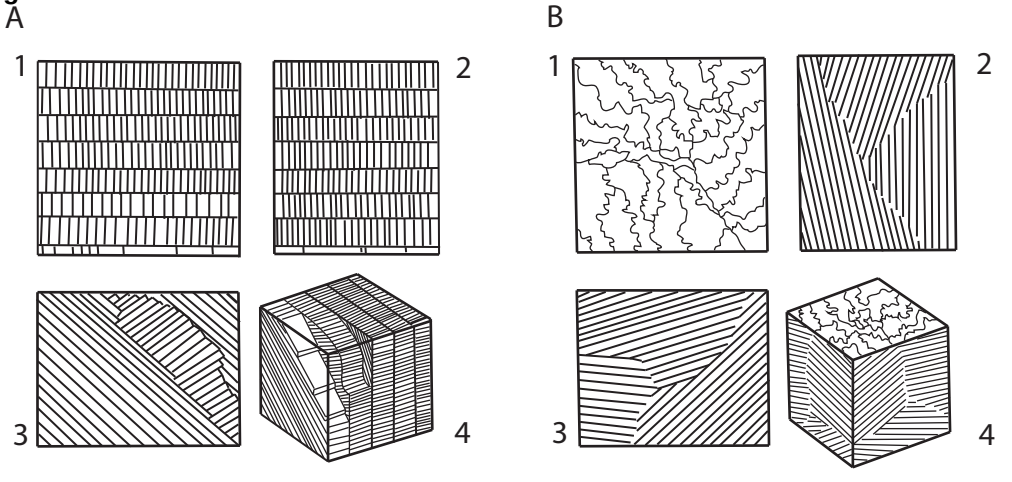

Figure

Click here to download high resolution image

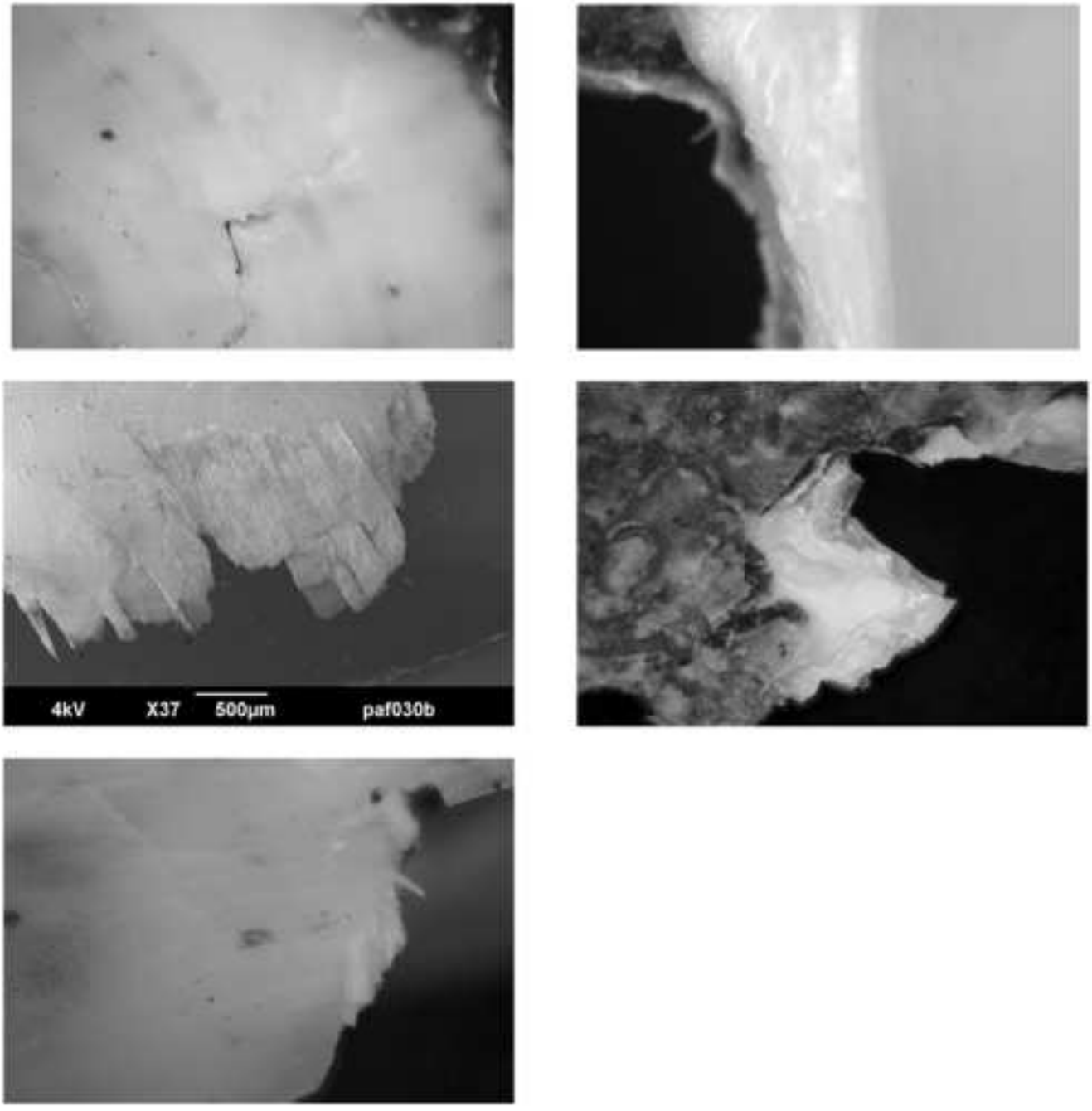

Figure

Click here to download high resolution image

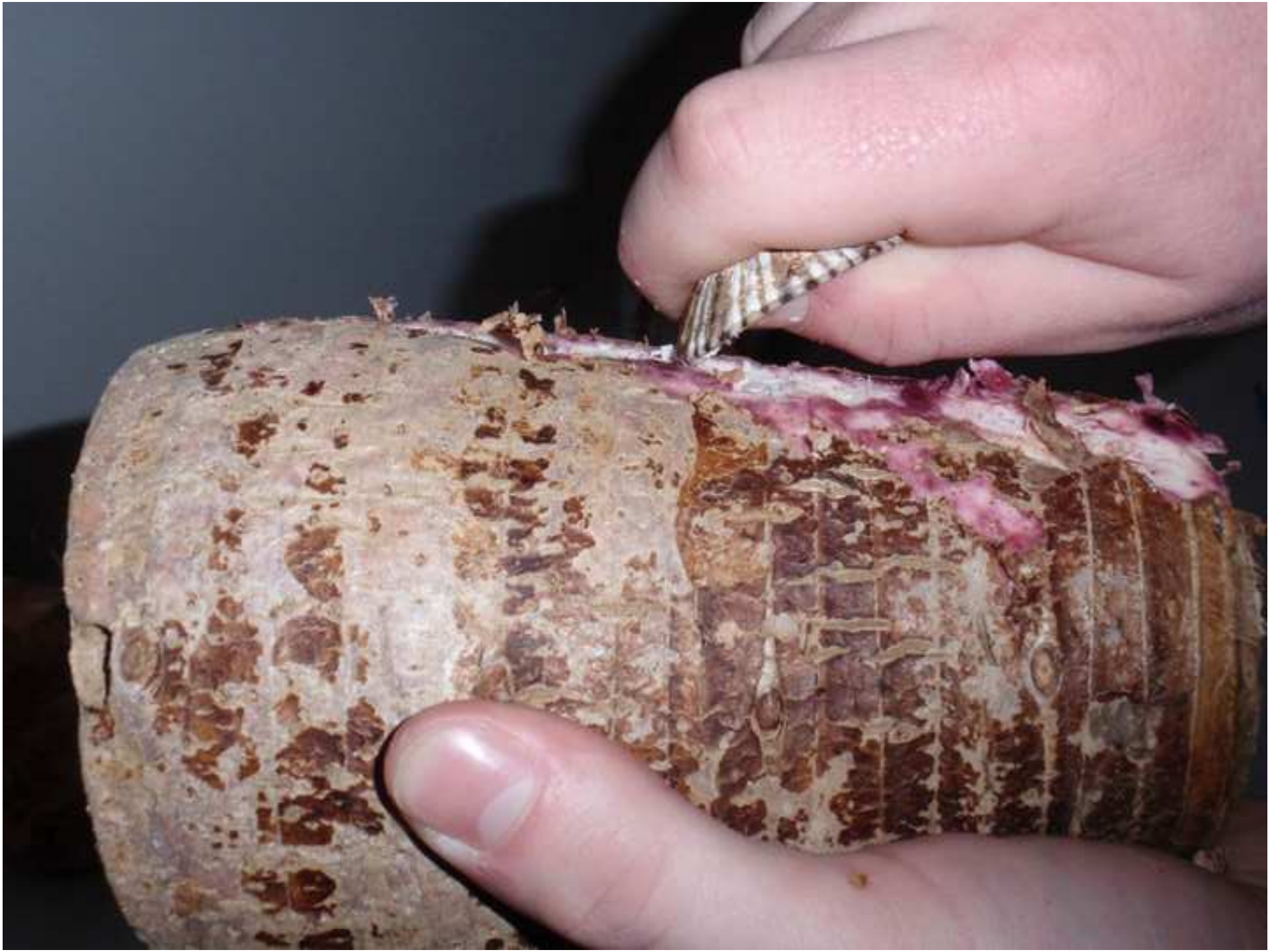

Figure

Click here to download high resolution image

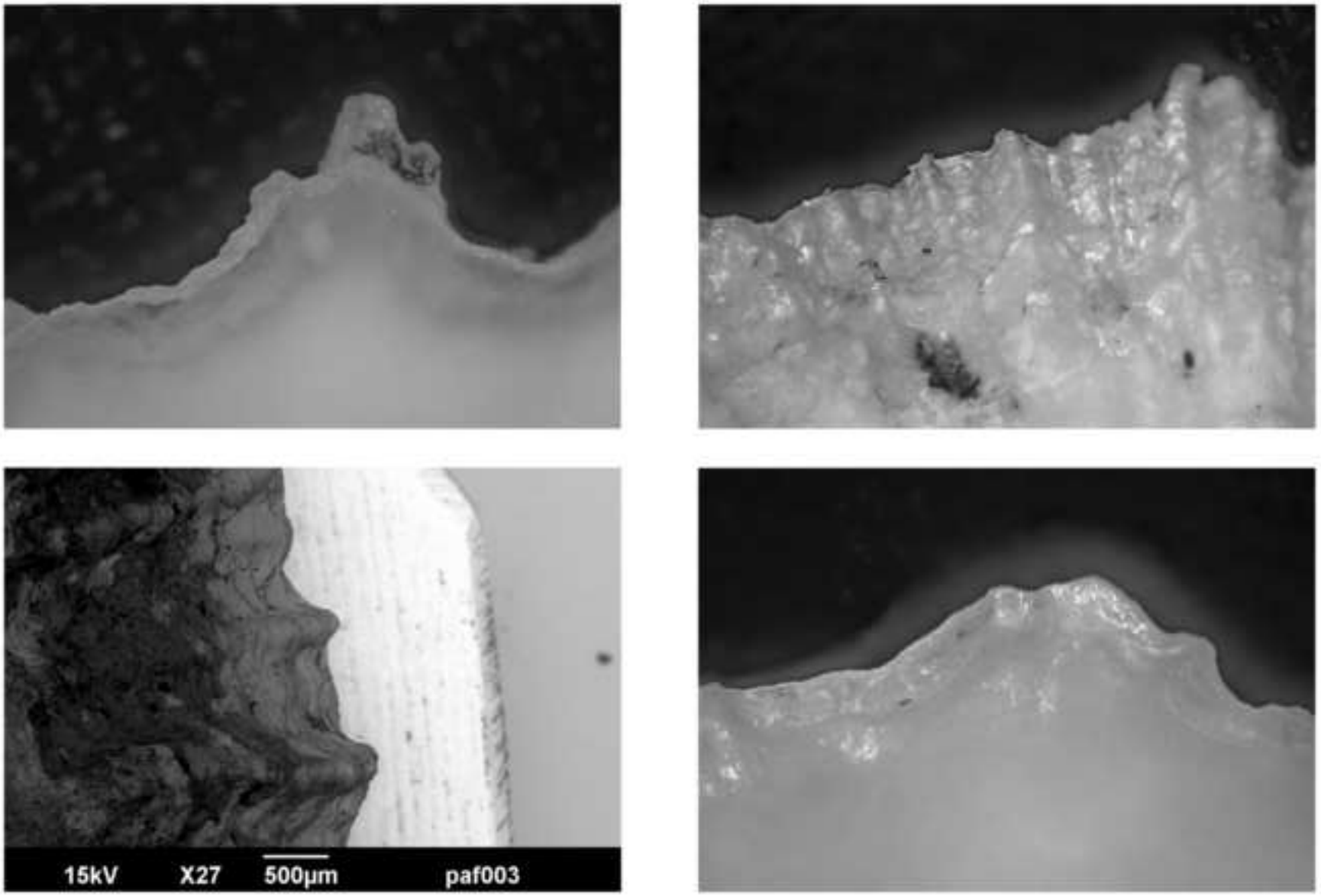

Figure

Click here to download high resolution image

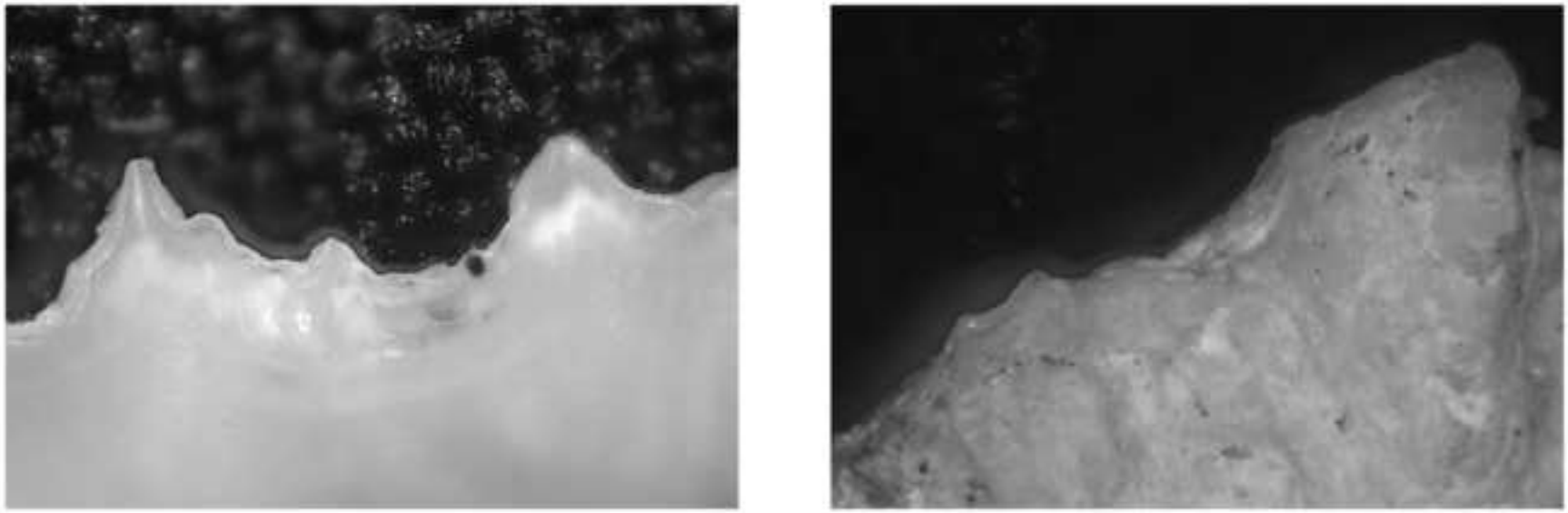

Figure

Click here to download high resolution image

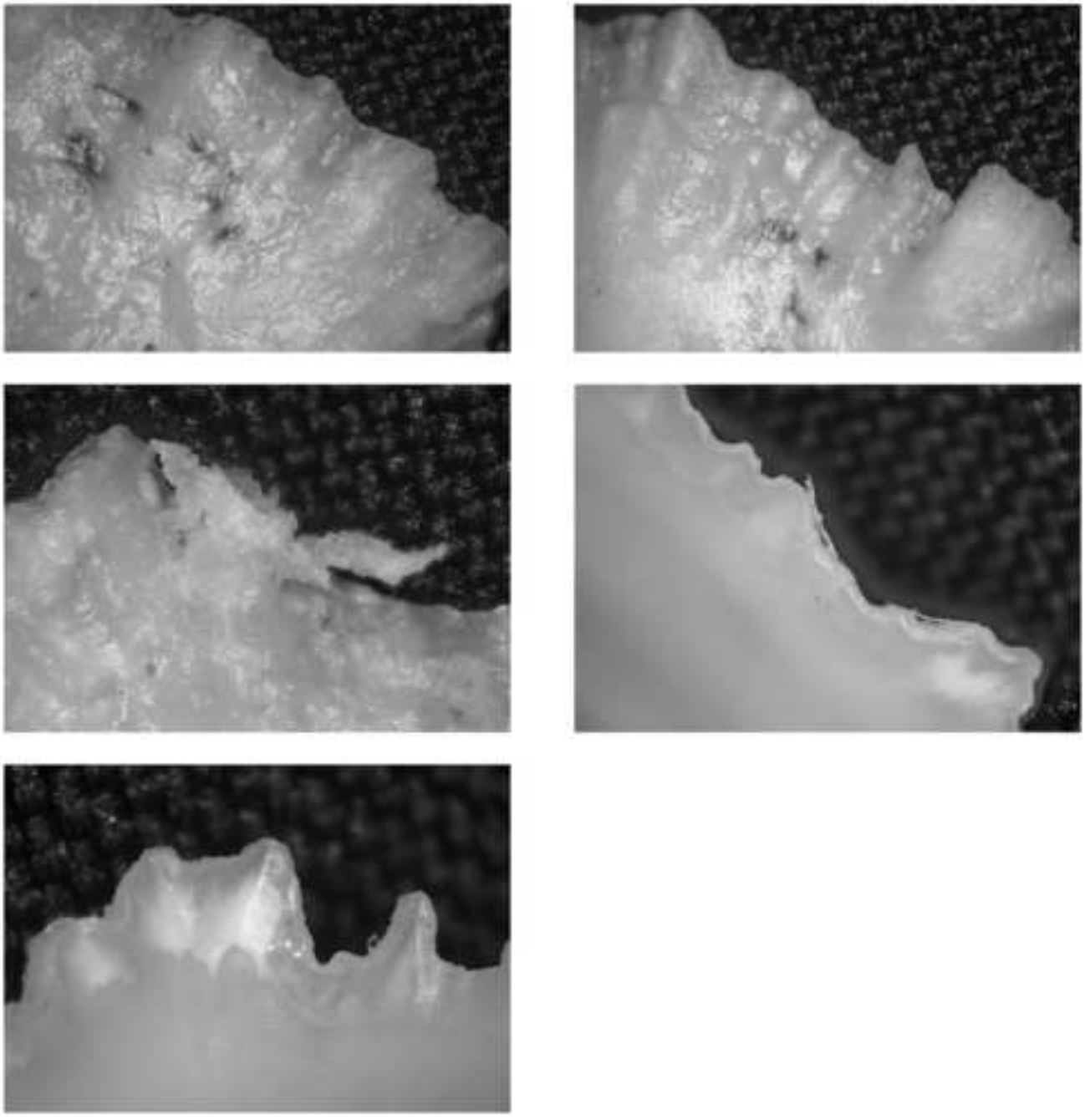

Figure

Click here to download high resolution image

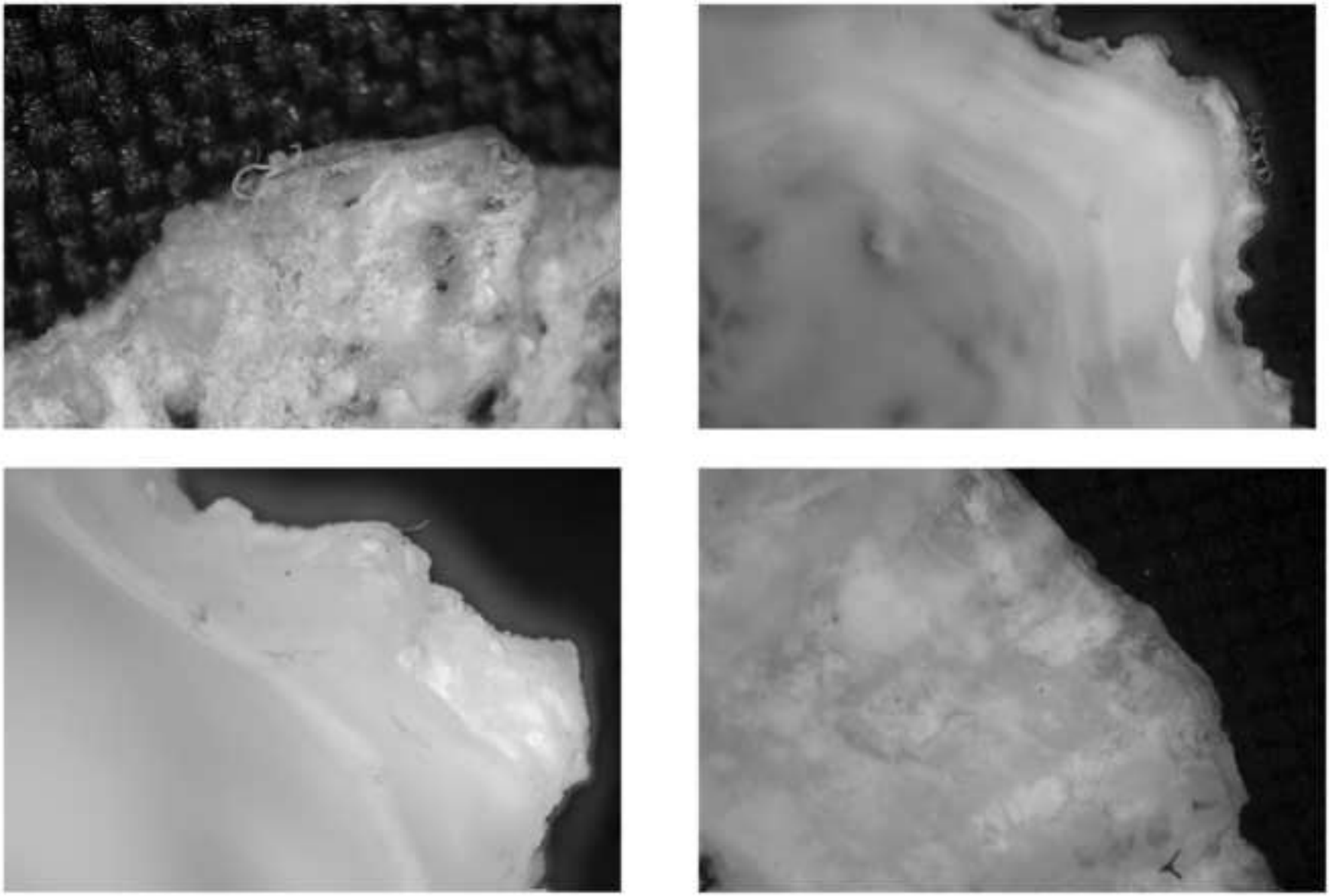

Figure

Click here to download high resolution image

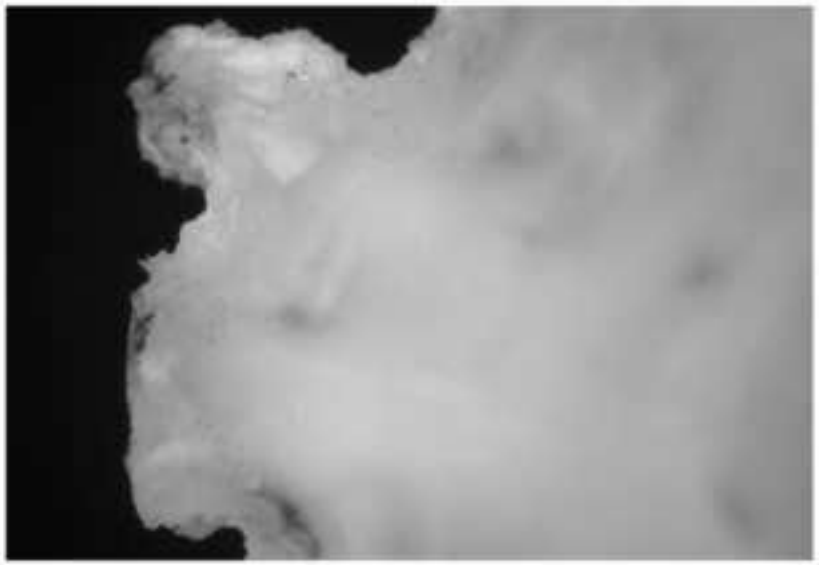

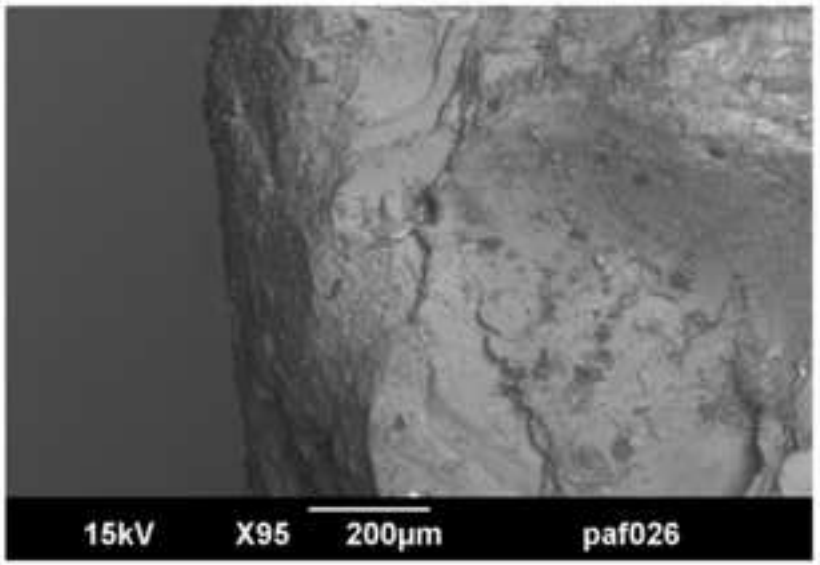

Figure

Click here to download high resolution image

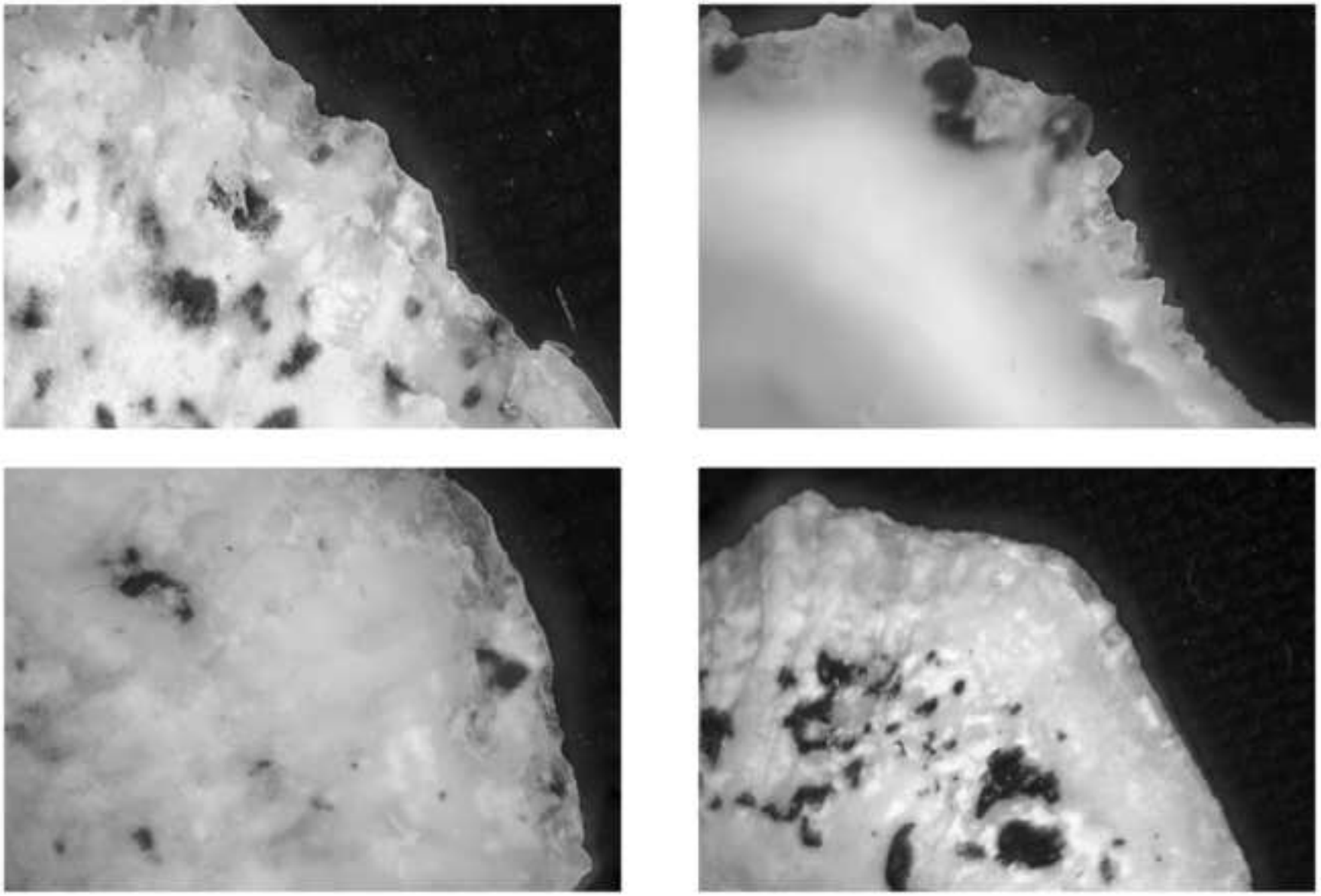

Figure

Click here to download high resolution image

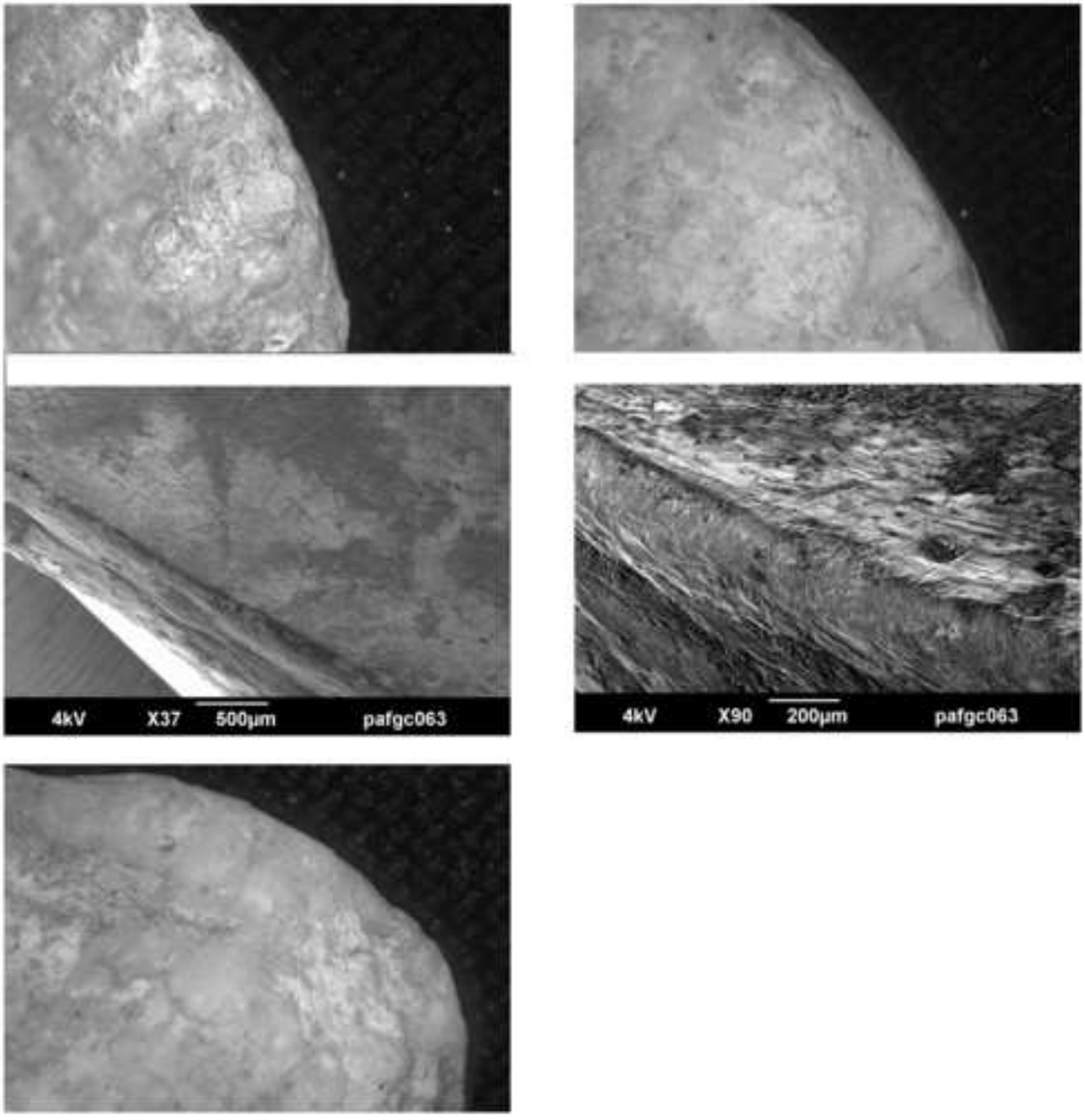

Figure

Click here to download high resolution image

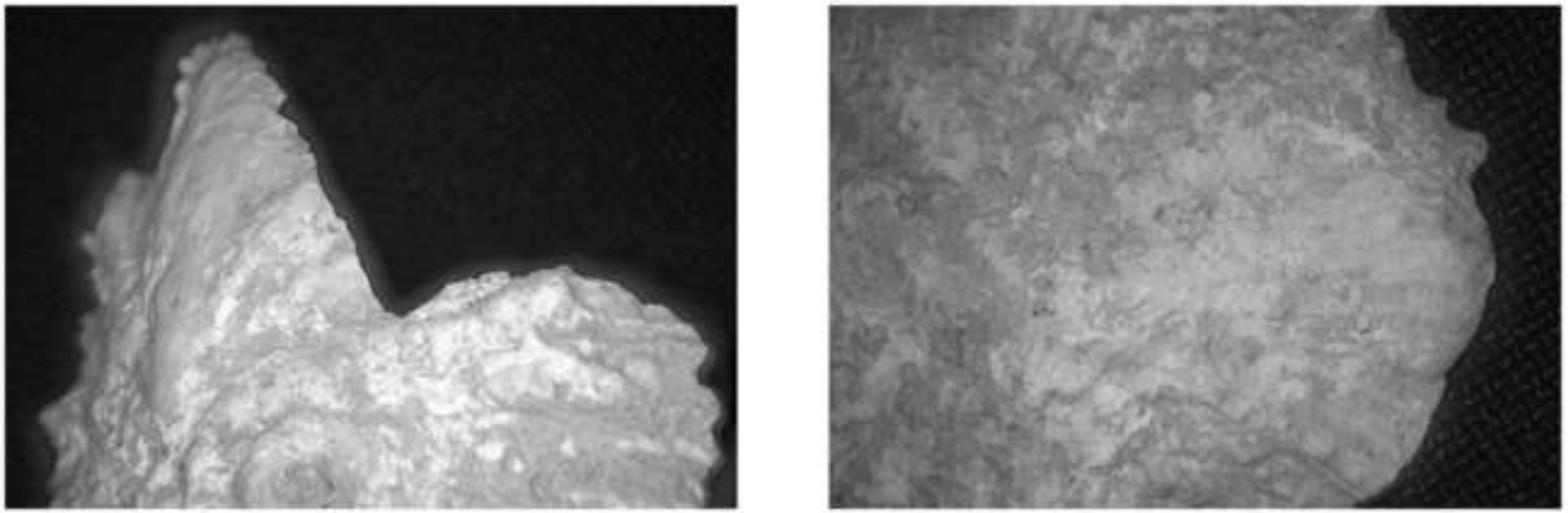

Golo Cave ms Captions

Figure 1: Map showing the location of Gebe Island and Golo Cave.

Figure 2: Archaeological *Scutellastra flexuosa* from Golo Cave showing dorsal, lateral and ventral views.

Figure 3: Golo Cave *Scutellastra flexuosa* with putative working noted during the original shell midden analysis. From Square M4, 200-205cm depth.

Figure 4: Schematic illustrations of crossed structures present in *S. flexuosa*. A: crossed lamellar structure; (1) inner surface (2) commarginal section (3) radial section (4) oblique three dimensional view. B: Irregular complex crossed foliated structure; (1) inner surface (2) commarginal section (3) radial section (4) oblique three dimensional view. Redrawn from Fuchigami and Sasaki (2005: figure 16).

Figure 5:

S. flexuosa used for simulated natural fracture experiments: (a) irregular crack radiating from the margin to the apex. Concentric fatigue fractures are also visible, 40x magnification; (b) Various diverse fracture paths of stacked layers in anterior-posterior compressive force delivery, 160x magnification; (c) Scanning electron microscope image of a fracture edge showing 'tearing' apart of bundles of crystals; (d) Various diverse fracture paths of stacked layers in lateral compressive force delivery, 40x magnification; (e) Fracture edge showing 'tearing' apart of bundles of crystals as well as multidirectional fracture paths, 80x.

Figure 6: Photo showing the way in which the *S. flexuosa* shells were gripped during working experiments – in this instance for the peeling of a taro corm.

Figure 7:

S. flexuosa used for taro peeling experiments: (a) microchipping at posterior margin, taro peeling 100x, 65x magnification; (b) the removal of shell from the exterior surface of the posterior margin, taro peeling 20x, 40x magnification; (c) Scanning Electron Microscope image of shell removal at the exterior posterior margin, taro peeling 20x; (d) microchipping and polish at the posterior margin, taro peeling 100x, 45x magnification.

Figure 8:

S. flexuosa used for yam peeling experiments: (a) microchipping at posterior margin, yam peeling 100x, 45x magnification; (b) removal of portions of outer layer of shell in furrows between ribs on exterior, yam peeling 100x, 55x magnification.

Figure 9:

S. flexuosa used for coconut flesh scraping: (a) glossy sheen across exterior surface, coconut scooping 100x, 40x magnification; (b) muting of exterior surface sculpture, coconut scooping 100x, 40x magnification; (c) chipping at margin, coconut scraping 100x, 40x magnification; (d) microchipping at margin, coconut scooping 100x, 50x magnification; (e) opaque patches at margin as a result of pressure exerted on the shell's edge, coconut scooping 100x, 50x magnification.

Figure 10:

S. flexuosa used for scraping the interior and exterior of soaked and dry bamboo culms: (a) faceting and residue at margin, dry bamboo exterior scraping 100x, 45x magnification; (b) concentric fatigue fractures visible on interior shell surface, dry bamboo exterior scraping 100x, 20x magnification; (c) microchipping at margin, soaked bamboo interior of culm 100x, 80x magnification; (d) muting of exterior surface sculpture, soaked bamboo exterior of culm 100x, 50x magnification.

Figure 11:

S. flexuosa used for scraping a nodule of haematite: (a) faceting and accumulation of residue at margin, haematite scraping 20x, 45x magnification; (b) Scanning Electron Microscope image of facet and adhering residue, haematite scraping 20x. The small highly reflective particles on the surface are fragments of powdered haematite.

Figure 12:

S. flexuosa used for cutting pig skin: (a) flaking of exterior shell layers, pig skin cutting 100x, 50x magnification; (b) translucence at margin from material lost on outer surface, pig skin cutting 100x, 55x magnification. *S. flexuosa* used for cutting pig flesh: (c) flaking and splintering of shell at margin resulting in translucence. Also loss of sculpture on body surface, 55x magnification. *S. flexuosa* used for scraping pig bone: (a) margin attrition and zone of exterior smoothing, pig bone scraping 100x, 30x magnification.

Figure 13:

S. flexuosa shells from Golo Cave with edge-rounding and faceting: (a) Specimen PafGC023, from Square M4 185-190cm depth. Rounding and faceting of fractured shell posterior with attritional wear on elevated sculpture but not in intervening furrows, 50x magnification; (b) Specimen PafGC063, from Square M4 200-205cm. Rounding and faceting of fractured shell posterior edge, 40x magnification; (c) Scanning Electron Microscope image of PafGC063 worked edge showing even shell removal and lack of chipping, tearing of differential wear across layers; (d) Scanning Electron Microscope image of PafGC063 showing the different orientations of shell within the fracture edge cross-section and the even removal of each through abrasion; (e) Specimen PafGC008, from Square M4 200-205cm depth. Rounding

across edge with irregular outline and removal of shell material in a band back from the working edge, 40x magnification.

Figure 14

S. flexuosa shells from Golo Cave with abrasion to localised patches on the dorsal surface: (a) Specimen PafGC015, from Square M4 200-205cm depth. Abrasion and muting of sculpture of the main elevated posterior rib, 15x magnification; (b) Specimen PafGC041, from Square M4 205-210cm depth. Abrasion and muting of sculpture on one of the main anterior radial ribs, 20x magnification.

Table 1: Radiocarbon results by square and depth. Recalibrated from Bellwood et al. (1998) with the addition of recently acquired determinations. Calibrated using Calib 7.0.2 with the Marine13 calibration data set for shell and the IntCal13 data set for charcoal (Stuiver and Reimer 1993). A ΔR value of 0 has been used for shell samples as has been recommended for this region (F. Petchey, personal communication, 2007).

Table 2: Pleistocene shell midden species list and MNI data for Square M4, 175-250 cm depth range. A further forty-eight taxa from this square and depth range were identified where MNI equals less than five. *Denotes landsnail species.

Table 3: Table outlining the experimental materials, actions and durations.